

1406

AISC E&R Library



The Behavior of Trusses With Eccentric Joints

By

Timothy J. Connelly

Carl E. Kirt — author

key words:

- 1- truss members
- 2- connections

A Report on Research Sponsored by
The American Institute of Steel Construction
and
Havens Steel Company

University of Kansas
Lawrence, Kansas
October 1990

RR1406

7550

4
1
2
3
4
5
6
7
8
9
10
11
12
13
14
15
16
17
18
19
20
21
22
23
24
25
26
27
28
29
30
31
32
33
34
35
36
37
38
39
40
41
42
43
44
45
46
47
48
49
50

**The Behavior of Trusses
With Eccentric Joints**

By
Timothy J. Connolly
Carl E. Kurt

A Report on Research Sponsored by
The American Institute of Steel Construction
and
Havens Steel Company

University of Kansas
Lawrence, Kansas
October 1990

Abstract

Truss systems are usually designed based on the assumption that they have concentrically loaded joints. However, many design situations require the evaluation of joint eccentricity. An examination of the literature on the subject offers very little guidance to the engineer and fabricator in the establishment of specific design and analysis guidelines.

Tests were conducted on five steel trusses to evaluate member response and overall truss stiffness due to the effects of joint eccentricities. Joint eccentricities ranging from zero to four inches were selected to be representative of eccentricities that could typically occur during the fabrication process without detection.

The measured ultimate load carrying capacity and overall truss stiffness for the trusses investigated in this study were compared with theoretical predictive models. Recommendations are made to aid in the analysis of trusses with eccentric connections.

The test program and the analytical study indicated that for trusses of similar geometry and load conditions, large joint eccentricities can have a detrimental effect on the behavior and ultimate capacity of a planar "truss" structure.

Acknowledgments

I would like to express my appreciation to the American Institute of Steel Construction for their financial support for this research project. I would like to thank Mr. Bill Richey, of Havens Steel Company, for his assistance during this project. I would also like to thank Havens Steel Company for supplying the test specimens for this project.

A special thanks to Dr. Carl Kurt for his guidance and counsel during my studies and his assistance throughout this project.

Timothy J. Connolly

Table of Contents

	<u>Page</u>
Chapter 1 - Introduction	1
1.1 Statement of Problem	1
1.2 Objectives and Scope	2
1.3 Organization of Thesis	2
Chapter 2 - Literature Review	4
2.1 General	4
2.2 Secondary Stresses	6
2.3 Unbalanced Welded Connections for Angle Tension Members .	7
2.4 Shear and Tension in Welded Truss Connections	8
2.5 Compression Chords of Steel Joists	10
2.6 Predicting the Behavior of Trusses	12
2.7 Torsional-Flexural Buckling of Singly Symmetric Sections ...	16
2.8 Conclusion	18
Chapter 3 - Experimental Investigation	20
3.1 General	20
3.2 Test Specimen	20
3.3 Material Properties	27
3.4 Specimen Preparation	28
3.5 Load System	31
3.6 Instrumentation	33
3.7 Test Procedure	33

	<u>Page</u>
Chapter 4 - Experimental and Analytical Results	39
4.1 Truss Specimen Behavior	39
4.2 Analysis of Member End Forces	49
4.2.1 Experimental Determination of Member End Forces .	49
4.2.2 Theoretical Determination of Member End Forces ...	57
4.2.3 Comparison of Experimental and Analytical Member End Forces	58
4.3 Ultimate Load Capacity Comparisons	65
4.4 Truss Stiffness	77
4.5 Conclusions	79
Chapter 5 - Conclusions and Recommendations	83
5.1 Summary and Conclusions	83
5.2 Design and Analysis Recommendations	85
5.3 Recommendations for Further Work	87
References	88

List of Figures

<u>Fig. No.</u>	<u>Title</u>	<u>Page</u>
2.1	Typical Eccentric Welded Connection	9
2.2	Loading Paths of Hypothetical Members	15
3.1	Truss Specimen with Design Bar Forces	22
3.2	Details of Truss Specimen #1	23
3.3	Eccentric Joint Configurations	25
3.4	Typical Coupon Stress Strain Curve	29
3.5	Loading System	32
3.6a	Gauge Locations Truss #1	34
3.6b	Gauge Locations Truss #2, 3, & 5	35
3.6c	Gauge Locations Truss #4	36
4.1a	Failure Truss #1	40
4.1b	Failure Truss #2	41
4.1c	Failure Truss #3	42
4.1d	Failure Truss #4	43
4.1e	Failure Truss #5	44
4.2	Applied Load vs. Deflection Curves	46
4.3	Ultimate Load vs. Top Chord Eccentricity	48
4.4a	Normal Strain Distributions Center-Line Joint U3	50
4.4b	Shear Strain Distributions Center-Line Joint U3	50
4.4c	Normal Strain Distributions Member U2-U3 at Joint U3	51
4.4d	Normal Strain Distributions Member U3-U4 at Joint U3	51
4.4e	Normal Strain Distributions Center-Line Joint L4	52

<u>Fig. No.</u>	<u>Title</u>	<u>Page</u>
4.4f	Shear Strain Distributions Center-Line Joint L4	52
4.4g	Normal Strain Distributions Member L3-L4 at Joint L4	53
4.4h	Normal Strain Distributions Member L3-L4 at Joint L4	53
4.5	Typical Strain Distributions for Member Force Calculations . . .	55
4.6a	Axial-Moment Interaction Diagrams - Truss #1	68
4.6b	Axial-Moment Interaction Diagrams - Truss #2	68
4.6c	Axial-Moment Interaction Diagrams - Truss #3	69
4.6d	Axial-Moment Interaction Diagrams - Truss #4	69
4.6e	Axial-Moment Interaction Diagrams - Truss #5	70
4.7a	Typical Joint Distortion - Concentric Top Chord Joint	80
4.7b	Typical Joint Distortion - Eccentric Top Chord Joint	80
4.7a	Typical Joint Distortion - Concentric Bottom Chord Joint	81
4.7b	Typical Joint Distortion - Eccentric Bottom Chord Joint	81

List of Tables

<u>Table No.</u>	<u>Title</u>	<u>Page</u>
3.1	Truss Specimen Joint Eccentricities	26
3.2	Average Material Yield Stress	30
3.3	Cross-Section Dimensions and Geometric Properties	37
4.1a	Member Forces Truss #1	59
4.1b	Member Forces Truss #2	60
4.1c	Member Forces Truss #3	61
4.1d	Member Forces Truss #4	62
4.1e	Member Forces Truss #5	63
4.2	Experimental and Theoretical Ultimate Load Carrying Capacity	66
4.3	Truss Stiffness	78

Chapter 1

Introduction

1.1 Statement of Problem

A truss is a commonly used structural configuration designed to resist transverse loads. A truss is typically formed by a system of structural members arranged in triangles or groups of triangles, joined together at their ends to form a stable framework. The truss members are typically designed for pure tensile or compressive forces.

Tee sections for the top and bottom chords with double angle web members fastened directly to the stem of the tee chord is a common type of light truss construction and is considered in this study. The tee sections, cut from rolled shapes, are often used for the chords of light trusses. The tee sections are light weight, and the tee stems can be used for connecting the web members without the use of a gusset plate.

Truss systems are usually designed based on the assumption that they have concentrically loaded joints. To avoid eccentricity at a joint, the line of action of the load from each member framing into a joint should intersect at the joint centroid. However, because of fabrication tolerances, member straightness, and connection methods, many design situations require the evaluation of joint eccentricity.

It is desirable and necessary to know accurately the load carrying capacity of a structure with such imperfections. However, an examination of the literature on the subject offers very little guidance to the engineer and fabricator in the establishment of reasonable alignment tolerances for truss members. In some situations, lack of specific design and analysis guidelines may result in unnecessary and expensive reworking of fabricated trusses.

1.2 Objectives and Scope

This investigation deals with the behavior of simple, planar trusses with misaligned members. The trusses were fabricated with intentional eccentricities ranging from zero to four inches at the interior panel points.

The objectives of this investigation are to:

- 1) develop and conduct a test program to study the in-plane effects of joint eccentricities in simple planar trusses;
- 2) conduct an analytical study to evaluate and compare the results of the experimental test program;
- 3) present a recommended procedure for evaluating the effects of joint eccentricity in trusses.

1.3 Organization of Thesis

Chapter 2 describes past experimental research involving eccentric truss connections. Chapter 3 contains descriptions of the testing procedures, the test fixture, and the test specimen. The experimental data and data analysis are

presented in Chapter 4. Chapter 5 is a summary of conclusions reached through this investigation and recommends future research topics.

Chapter 2

Literature Review

2.1 General

There are three fundamental assumptions made in the analysis of idealized planar trusses. They are: 1) All members are connected at their ends with frictionless pins; 2) The loads and reactions are applied at the truss joints only; 3) The centroidal axis of each member is straight and coincides with the line connecting the joint centers at each end of the member [West 1989]. In reality, truss type structures normally do not meet these basic assumptions.

If the above assumptions are true, each truss member will carry only axial load and no bending moments or transverse forces will be present. Because each member theoretically acts as a simple bar, truss analysis and design is relatively straight forward. In practical cases, however, no member is truly pin connected at its ends. Most truss connections are bolted or welded and frequently the chords are fabricated of members continuous through the joint.

The methods of connecting truss members has changed with time. Pin connections were replaced with less expensive riveted connections in the 19th century. This gave rise to the use of continuous chords, providing continuity of

01436

the member through the joints for ease of connection. As welding became accepted as an efficient and reliable method of connection, concerns of the effects of unbalanced welds as well as the increased rigidity of the connection became an issue. However, it has been suggested that bending stresses due to continuity and method of connection are unlikely to affect the ultimate capacity of the truss subjected to non-cyclic loading conditions [Parcel and Murer 1936]. While continuity of the chord and rigidity of the connection introduce secondary stresses, the effects tend to be canceled. The increased joint stiffness produces secondary bending stresses in the members framing into the joint. However, compression members within a truss are typically conservatively designed as pin-ended members rather than a beam-column with joint stiffness. Tension members made of ductile material have the inherent ability to adsorb secondary stresses through local yielding and deflection without stability becoming a concern. Thus, the assumption of pinned ends gives reasonably good results for most truss type connections [West 1989].

The second assumption that loads and reactions act at truss joints is easily met if proper attention is given to the details of load paths. However, if loads are introduced between joints, the truss should be designed as a "frame" to account for bending moments and shear forces.

The third assumption of straight members and concentric joints requires that eccentricities be avoided within the truss system. An out-of-straight member is typically corrected after rolling to meet standard sweep and camber

01427

tolerances [AISC 1989]. Individual members can be cambered at the time of fabrication to account for dead load deflections to provide a "straight structure". If a member is significantly out-of-straight, the analytic and design procedures must account for any additional induced stresses. To avoid eccentricity within a joint, the centroidal axes of all members framing into a joint are to intersect at a common point within the connection. This assumption can typically be fulfilled by careful detailing and reasonable fabrication tolerances. However, when unacceptable imperfections do arise, they must be accounted for in the analysis.

2.2 Secondary Stresses

An analysis utilizing the assumptions of an ideal truss will provide the primary bar forces in the truss members. Forces within the truss structure due to variance of the ideal assumptions are considered to differ from the primary bar forces and are called secondary bar forces. However, in most cases secondary forces in steel trusses may be neglected without structural concern. It is important, though, that secondary forces be defined properly and the analysis and design be consistent with each other.

Additional stresses, which result from structural differences between the actual truss and the analytical model, are regarded as secondary stresses. For example, if the truss members are designed for axial forces that would result if the member ends were pin connected, then all other stresses which are not due to the axial forces in the members are considered secondary stresses.

However, if the axial forces for member design are determined using an analysis including flexural effects, the flexural effects in the analysis may have reduced the axial forces indicated by the analysis. In this case, the flexural stresses may not be dismissed as secondary stresses [Nair 1988].

Some engineers prefer the definition that secondary stresses are only the flexural stresses resulting from truss member continuity at the nodes of a truss with a concentric connections [Korol 1986]. This definition leaves less to question and will be used within this thesis. This implies that stresses due to joint eccentricities are primary and must be included in the member design. When unacceptable flexural stresses are found, the "truss" should be analyzed and designed as a "frame" considering axial, flexural and shear forces.

2.3 Unbalanced Welded Connections for Angle Tension Members

A test program was conducted by Gibson and Wake [1942] to investigate the effects of eccentricities due to unbalanced welded connections for angle tension members. The practice of balancing welds consists of distributing the welds along the heel and toe of the angle such that the working strengths of the welds are balanced about the projection of the center of gravity of the angle on the connected leg. It is often difficult or expensive to provide space for such connections. Thus, the study sought to determine whether it was necessary to conform to the theoretical balanced design or whether other arrangements of welds are equally effective.

The test specimens consisted of two angles $2\ 1/2 \times 2\ 1/2 \times 5/16$ cut to

length and fitted to grip plates in a jig so that the center of gravity of the angle and the center line of each grip plate were in a plane normal to the connection. Fifteen different arrangements of welds were investigated, representing most of the types of joints commonly used for statically loaded angle connections. The results showed:

"that there is no advantage in strength of the balanced connection when compared to the unbalanced connection... The conventional theory that the working strengths of the welds connecting an angle member must be balanced about the projection of the center of gravity of the angle on the connected leg is, therefore, not essential to the design of adequate connections for angle tension members" [Gibson and Wake 1942].

As can be seen from Figure 2.1, angles with relatively short legs will have small eccentricities produced by unbalanced welds. Thus, the results of Gibson and Wake's test program are applicable for tension members with small eccentricities, because tension members made of ductile material can typically redistribute the resulting secondary stresses by local yielding or deflection without significant reduction of carrying capacity.

2.4 Shear and Tension in Welded Truss Connections

Experimental and analytical work for the truss tee chords with double angle web member type connection has been carried out at the University of New Brunswick [Walton 1979, Dawe et al. 1985]. Over thirty full-scale welded truss connection specimens were tested to determine the effects of various factors influencing this type of connection. Walton conducted an experimental

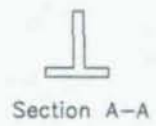
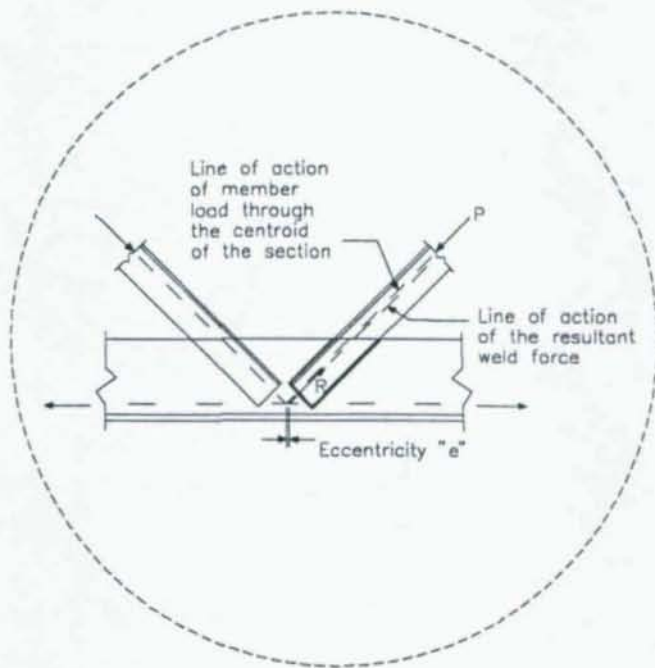
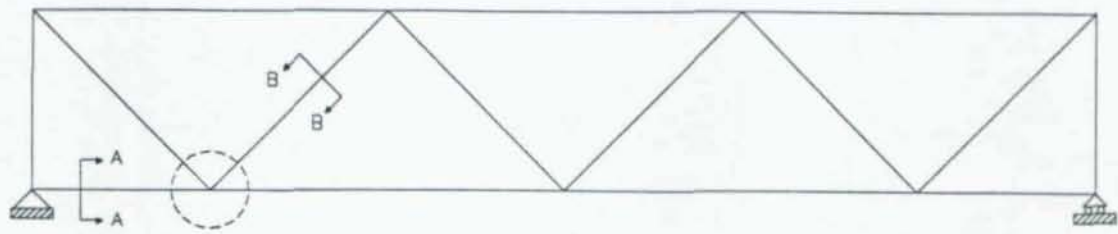


Figure 2.1 Typical Eccentric Welded Connection

program to determine the possibility of over stressing the tee stem within the connection due to high combinations of shear and tension. A series of full-scale welded truss connection specimens were investigated. Other parametric considerations such as the effects of inclination of a diagonal web member as well as intentional joint eccentricities were later investigated by Dawe & Pond.

The results of the experimental programs indicated that the angle of inclination of the web members had little or no influence on the capacity of the connection and that positive joint eccentricities, due to member misalignment, of the magnitude investigated (0.12", 1.0", 1.9", and 2.4") had no detrimental effect on the ultimate capacity of the connections being investigated. Positive eccentricity being defined as the cases in which the force lines of the web members intersect above the centroid of the chord cross-section in the stem or flange of the section. In fact, the investigators felt there was some indication that joints with positive eccentricities behaved in a more ductile manner and had somewhat increased ultimate capacities over similar non-eccentric joints. However, the test specimens used at the University of New Brunswick consisted of a single truss joint with a critical failure mode of combined shear and tension in the stem of the connection and not an entire truss specimen.

2.5 Compression Chords of Steel Joists

Research has been conducted to aid in the optimal design of the top chord of open web steel joists. In the 1960s, an investigation was conducted at the University of Kansas to study the behavior of the compression chord of full

scale open-web steel joists [Lenzen 1968]. Loading conditions consisted of concentrated loads in the central position of the joist or uniform load along the length of the compression chord. The study sought to establish the acceptability of various compression formulas for the design of the compression chords of steel joists. The moments at the center of the compression chord due to joint eccentricity, uniform load, restrained ends and axial load were evaluated. The joint eccentricities investigated were generally small as a result of member misalignment due to the method of connecting the web material to the chords.

An empirical interaction formula was developed and showed good agreement with the test results. The study found the following equation to be representative of the compression chord behavior for the open-web steel joist tested:

$$\frac{P}{A \sigma_{TM}} + \frac{MC}{I \sigma_{YS}} = 1.0 \quad (2.1)$$

in which

P = axial load

A = cross-sectional area

σ_{TM} = tangent-modulus stress

M = moment at center of compression chord

I = moment of inertia about the axis of bending

C = distance to the extreme compressed fiber due to bending

σ_{YS} = yield stress.

01443

Although Lenzen presented equation 2.1 as predictive of the beam-column behavior of the chords for floor joists, it was suggested that the equation not be implemented for design due to the similarity to and accuracy of the Allowable Stress Design [AISC 1989] combined stress equations. Equation 2.1 incorporated the tangent modulus stress theory to account for the effects of the non-linear stress-strain relationship of the material beyond the proportional limit on inelastic column buckling.

The Allowable Stress Design basic column-strength curve is based on the parabolic equation proposed by Bleich [1952]. However, the curve represents a compromise among column curves for various residual stress distributions. Thus, the parabolic curve adopted by AISC [1989] does not consider each member's individual stress distribution, but rather a generalized approximation of the effects of inherent material non-linearities on the ultimate strength of a column.

2.6 Predicting the Behavior of Trusses

Research has been conducted on the subject of predicting the behavior of statically indeterminate planar trusses [Korol et al. 1986]. A predictive model was formulated and compared with the test results of two concentric truss experiments.

The analytic model incorporated an incremental load procedure in a stiffness analysis to compute member forces and joint displacements at various stages of loading. The technique, applied to individual members, assumed

elastic perfectly plastic moment rotation characteristics that were dependent on axial load. Local buckling of a member was not considered, as the members of the trusses investigated were sections permitted in plastic design.

The model incorporated commonly accepted plastic design stability and strength interaction relationships for uniaxial bending, equations 2.2 and 2.3 respectively.

$$\frac{P}{P_{cr}} + \frac{C_m M}{M_m(1 - P/P_E)} = 1.0 \quad (2.2)$$

$$\frac{P}{P_y} + \frac{M}{1.18 M_p} = 1.0; \quad M \leq M_p \quad (2.3)$$

in which

P = axial load

P_y = yield strength of an axially loaded compression member

P_{cr} = maximum strength of an axially loaded compression member

P_E = Euler buckling load

M = maximum moment

M_m = maximum moment that can be resisted by the member in the absence of axial load

M_p = plastic moment

C_m = reduction factor to account for the critical location and magnitude of the secondary moment.

81445

The interaction relationships formed failure envelopes which were used to predict column buckling loads, the formation of plastic hinges, and the gross yielding of tension or compression members. The appropriate equations to investigate all pertinent failure modes must be considered in the model.

The following is a description of the principles of the model:

"To convey the essence of the method, suppose three elastic stress paths that represent force resultants at three locations in the truss are considered (Figure 2.2). Points A and B are associated with stocky struts; C pertains to a compression member of intermediate length. From Figure 2.2, point A marks the termination of elastic behavior. Points B and C are indicative of any elastic state. Subsequent loading has the effect of reducing the stiffness of the truss. This increase in load will require that stress point A follows [the failure envelope].

The next load increment is proportioned such that the next critical point, B, reaches the yield envelope to become B'. The associated stress points are A' and C'. Subsequent loading is incremented until the double primed points are reached. In this instance, buckling of member C occurs. Overall truss collapse would then result if the consequent shedding of C's load were not sufficiently compensated for by the reserve resistances available to the other members. Such a possibility would be likely if an array of plastic hinges had already formed to sufficiently reduce the structure's indeterminacy. Where this is not the case, there would be a step by step migration towards F caused by the axial forces' tending to increase in magnitude in concert with the progression of plastic hinging development during the loading history.

Once a member's stress state reaches point F, it is no longer capable of sustaining higher forces. This is equivalent to its removal from the structure and replacement by $p = \pm 1$ forces (tension or compression) acting on its joints" [Korol et al. 1986].

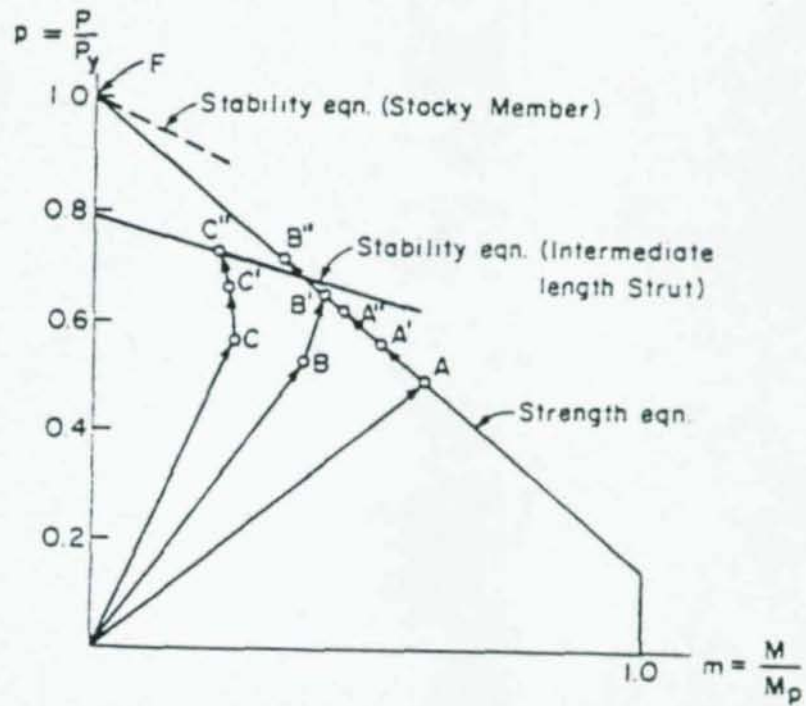


Figure 2.2 Loading Paths of Hypothetical Members [Korol et al., 1986]

91447

The computed ultimate capacities of the two trusses tested were within three percent of test results and the elastic stiffness predicted by the model almost exactly corresponded with those of the experiment.

Following the comparison of the analytic model with the test results, a parametric study considering the effects of varying joint eccentricity and truss depth was conducted. The analytic study concluded that small eccentricities have little influence on the truss ultimate load resistance and large eccentricities at the joints cause significant loss of strength.

2.7 Torsional-Flexural Buckling of Singly Symmetric Sections

Singly symmetric compression members such as the tee and double angle sections, within the type of truss construction being investigated within this study, can fail in one of the four following ways: 1) compression yielding---the maximum axial compressive load of the member, 2) flexural buckling---bending about an axis perpendicular to the axis of symmetry, 3) torsional-flexural buckling---bending and twisting about the axis of symmetry, or 4) plate buckling---local buckling of an element of the compression member.

Until the current edition of the AISC [1989] Allowable Stress Design specification, no explicit mention is made of the torsional-flexural buckling phenomenon which is important for singly symmetric sections. The current Allowable Stress Design specification [AISC 1989] does not provide a method for evaluating the torsional-flexural buckling stress of a member. However, the commentary for the AISC [1989] ASD method recommends the use of the AISC

[1986] Load and Resistance Factor Design specification to establish the effect of torsional-flexural buckling by the use of an effective column slenderness given by

$$\left(\frac{KL}{r}\right)_e = \pi \sqrt{\frac{E}{F_{e'}}} \quad (2.4)$$

When $(KL/r)_e$ is less than C_c , the allowable stress for torsional-flexural buckling is obtained from:

$$F_a = \frac{\left[1 - \frac{(KL/r)^2}{2C_c^2}\right] F_y}{\frac{5}{3} + \frac{3(KL/r)}{8C_c} - \frac{(KL/r)^3}{8C_c^3}} \quad (2.5)$$

and when $(KL/r)_e$ exceeds C_c , the allowable stress for torsional-flexural buckling is obtained from:

$$F_e = \frac{12\pi^2 E}{23(KL/r)^2} \quad (2.6)$$

where

$$C_c = \sqrt{\frac{2\pi^2 E}{F_y}}$$

$F_{e'}$ = as determined in the following LRFD analysis.

The LRFD method [AISC 1986] determines the nominal torsional-flexural critical stress F_{cr} as follows:

$$\text{for } \lambda_e \sqrt{Q} \leq 1.5$$

$$F_{cr} = Q(0.658^{\lambda_e^2}) F_y \quad (2.7)$$

for $\lambda_e \sqrt{Q} > 1.5$

$$F_{cr} = \left[\frac{0.877}{\lambda_e^2} \right] F_y \quad (2.8)$$

where

$$\lambda_e = \sqrt{F_y / F_{e'}}$$

$$F_{e'} = \frac{F_{ey} + F_{ez}}{2H} \left(1 - \sqrt{1 - \frac{4F_{ey}F_{ez}H}{(F_{ey} + F_{ez})^2}} \right)$$

- for a singly symmetric shape

$$F_{ey} = \frac{\pi^2 E}{(KL/r)_y^2}$$

$$F_{ez} = \left(\frac{\pi^2 EC_w}{(K_z L)^2} + GJ \right) \frac{1}{Ar_o^2}$$

The above equations assume the elements of the cross section under investigation meet width-thickness ratios as to preclude local buckling and therefore $Q = 1.0$.

2.8 Conclusion

Several important points are apparent from an overall evaluation of the information summarized in this chapter. First, the behavior of concentric rigid joint trusses is well known and documented. Second, it has been experimentally shown that small to moderate joint eccentricities do not have a

detrimental effect on the ultimate carrying capacity of a joint in tension and in some cases may be beneficial. Third, joint eccentricities can have a detrimental effect on the ultimate carrying capacity of the compression members of open-web steel joists.

Chapter 3

Experimental Investigation

3.1 General

Based on the previous information found in the literature review and the objectives of this study, an experimental test program was developed. Five statically determinate truss specimens were tested to determine the effects of member misalignment in simple planar trusses. Each truss was gauged with a series of strain gauges to determine the axial, shear, and moment forces at interior connections. The specimen configurations and test procedures will be discussed in the following sections. The test program was conducted in the Structural Engineering and Materials Laboratory at the University of Kansas.

3.2 Test Specimen

Each test specimen was fabricated using standard shop practices and was identical except for the degree of misalignment of the members about the work points of the interior connections. All trusses were 18 feet long and 3 feet deep with diagonal members at a 45 degree angle of inclination. The truss members were designed assuming concentric joints and fabricated from ASTM A36 material. The truss was designed to carry a concentrated tensile working load of 50 kips at joint L3. The design load of 50 kips was selected to keep the

ultimate load of the truss specimens within the capacity of the available load system. The truss configuration with design bar forces is shown in Figure 3.1.

In design practice, the desired mode of failure is yielding of a tension member. Thus, for a ductile material the failure mode is excessive deflection rather than a total collapse as would be associated with a stability failure. However, moments induced by joint eccentricity are typically more detrimental when acting on a compression member than on a tension member. Contrary to the behavior in compression members, tension members made of a ductile material such as structural steel conforming to ASTM A36 can compensate for secondary stresses induced by joint eccentricities by redistribution through local yielding or deflection. Therefore, to fully monitor the moment axial effects due to the eccentricity, the tension members were oversized to prevent overall member yielding. Lateral bracing was also provided to cause compression member with eccentric connection behavior to govern. The top and bottom chords for each truss were a WT 6 X 17.5. The diagonal web members were double angles 2 1/2 X 2 X 1/4 with their long legs back to back. To prevent premature failure away from the eccentric joints, the vertical end members were oversized using double angles 3 X 3 X 1/2. A bearing plate and stiffeners were placed at joint L3 to accommodate the load yoke and 1 inch thick bearing pads were placed at joints L1 and L5. A pin and a roller were used for the supports at joints L1 and L5, respectively. Details of a typical concentric truss specimen are shown in Figure 3.2.

All members framing into a connection are assumed to be connected at

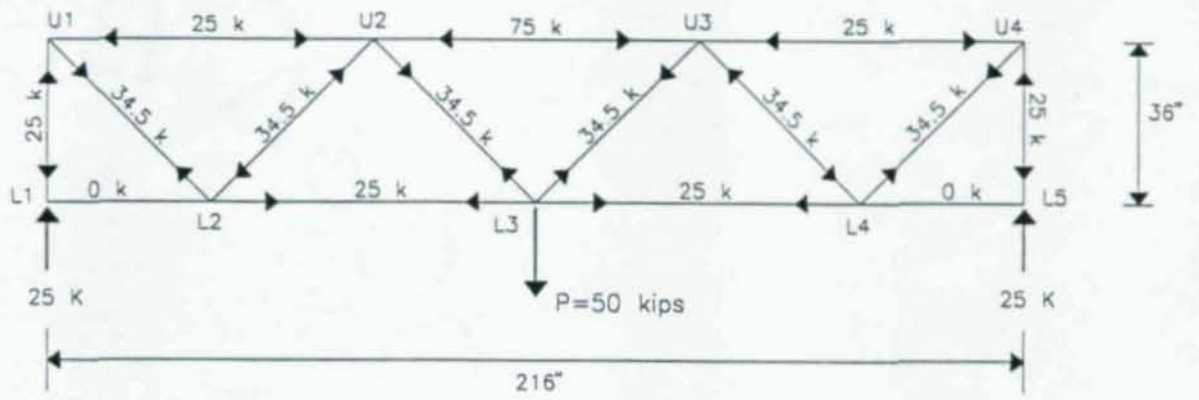
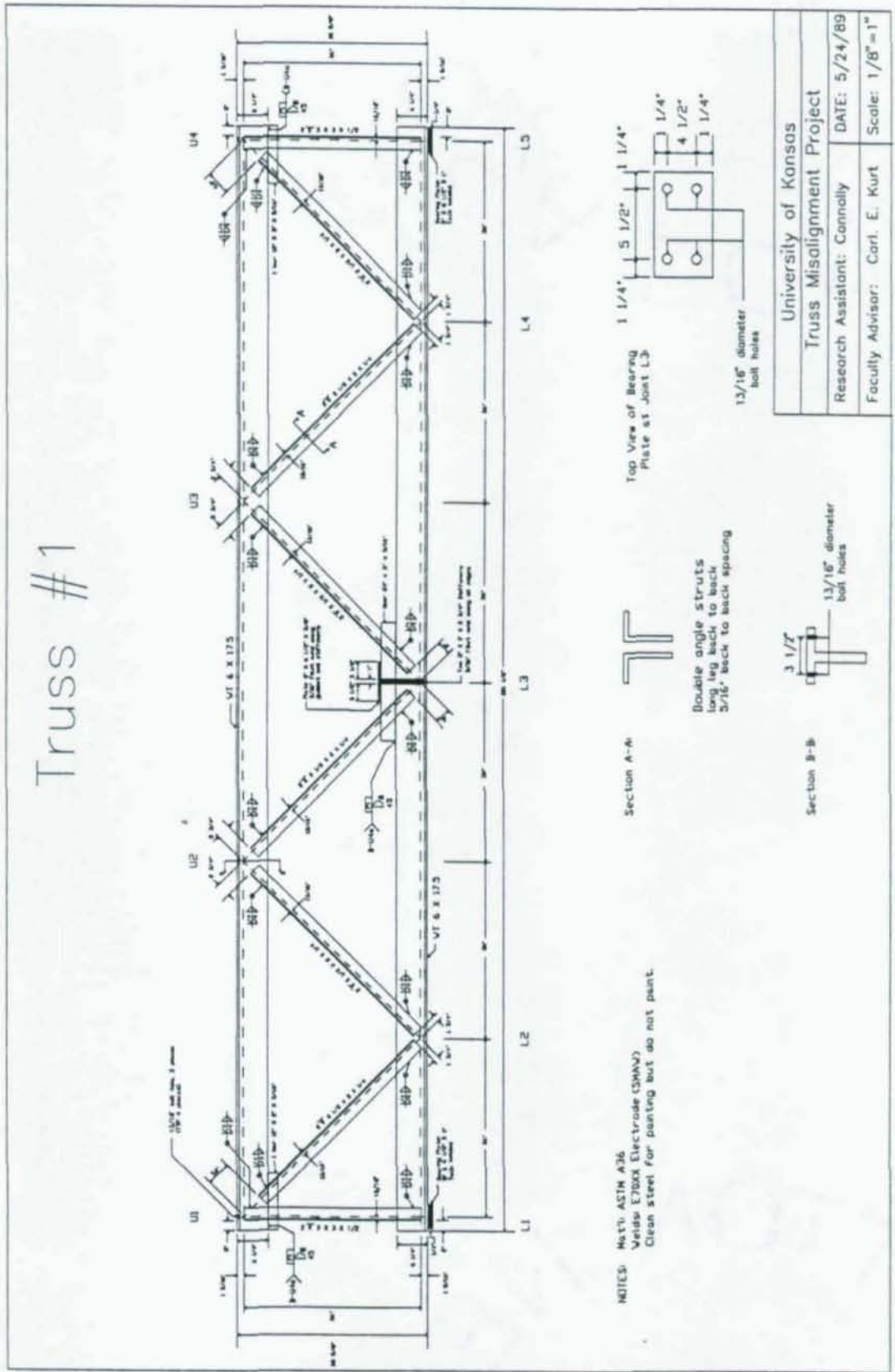


Figure 3.1 Truss Specimen with Design Bar Forces

Truss #1



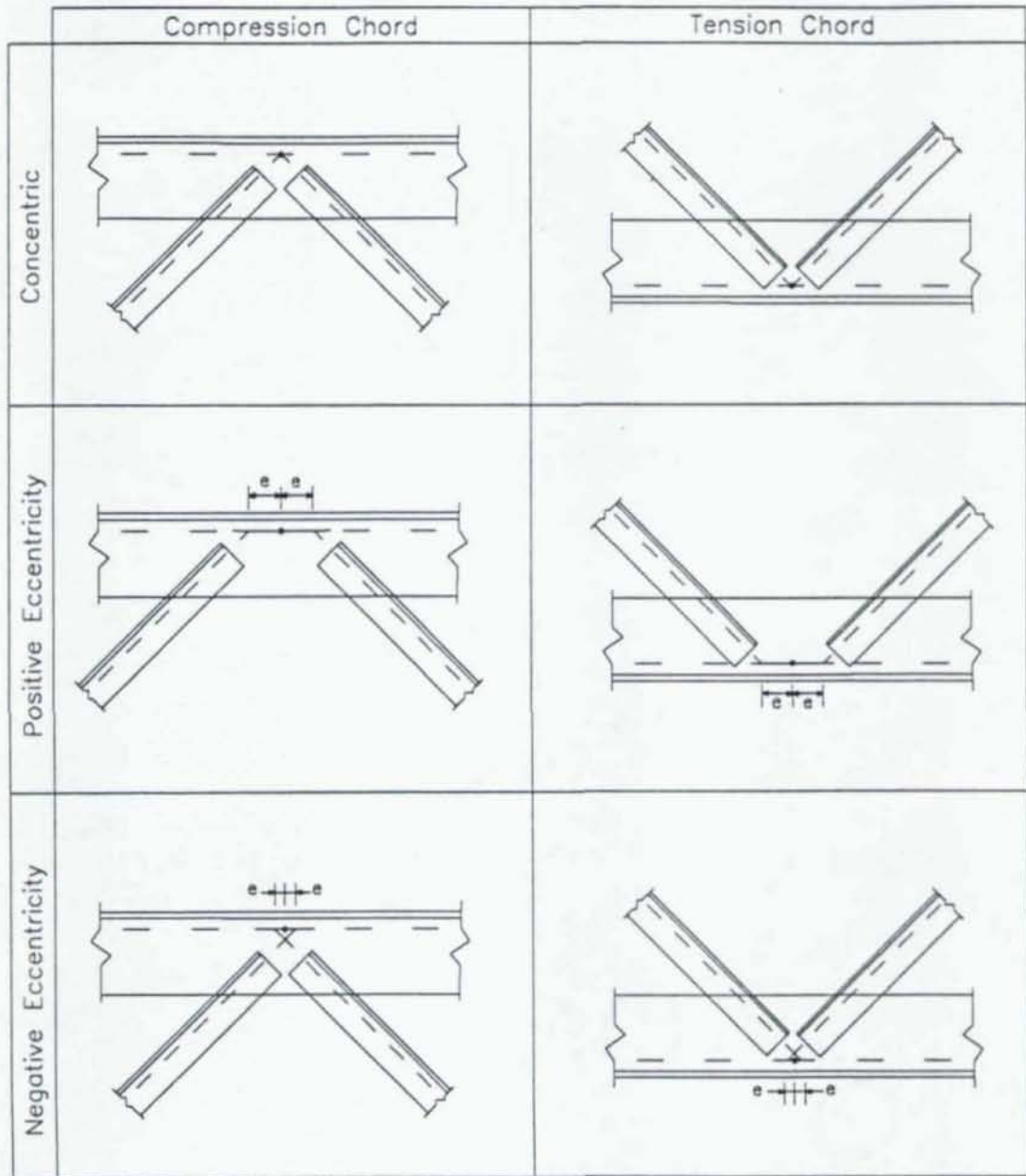
University of Kansas	
Truss Misalignment Project	
Research Assistant: Connolly	DATE: 5/24/89
Faculty Advisor: Carl E. Kurt	Scale: 1/8"=1"

Figure 3.2 Details of Truss Specimen #1

the joint work point (or work points in the case of an eccentric connection). The primary joint eccentricities about the theoretical work point of a concentric connection were due to member misalignment. Typical positive and negative eccentric joint configurations are illustrated in Figure 3.3. The eccentricity, e , of a member was measured as the horizontal distance from the theoretical work point of the joint to the intersection of the lines of action of the web member with that of the chord member. The truss specimens were designed to have equal eccentricities for each web member framing into an eccentric joint. Therefore, for example, a truss joint with a four inch eccentricity actually has a space of eight inches between the intersection of the lines of action of the web members with the line of action of the chord.

A range of positive eccentricities were studied in this test program. Connections are typically crowded to form a concentric connection and still have enough weld length connecting web members to the stem of the structural tee. Negative eccentricities were not modeled because it is much more probable for members to be misaligned with a positive eccentricity than with a negative eccentricity for this type of connection. It is often physically impossible to have a negative eccentricity of sizeable magnitude in an already "tight" connection. The magnitudes of joint eccentricity for each truss as built are listed in Table 3.1. Positive joint eccentricities ranging from zero to four inches were selected to be representative of eccentricities that could typically occur during the fabrication process without detection.

Lateral bracing was provided at each of the four top chord panel points



'•' -Theoretical work point for the joint.

Figure 3.3 Eccentric Joint Configurations

Truss	Joint U2	Joint U3	Joint L2	Joint L4
#1	0.25"	0.25"	0	0.25"
#2	2.0"	2.375"	0.25"	0.25"
#3	0.25"	0.375"	2.0"	2.0"
#4	4.0"	4.25"	0.875"	1.0"
#5	1.25"	1.375"	3.75"	3.875"

* Values to the Nearest 1/8"

** All Other Joints Nearly Perfect, Less Than 1/4" Eccentricity

Table 3.1 Truss Specimen Joint Eccentricities

01458

U1 through U4, and at the mid-height of both diagonal compression web members, struts L2-U2 and L4-U3. All lateral bracing members consisted of ASTM A36 2 X 2 x 1/4 angle. Lateral bracing was fastened to the flange of the top chord by two 3/4 inch A325 bolts. The lateral bracing at the mid-height of the diagonal compression members was fastened to the outstanding legs of the double angles with a 'C'-clamp. The outstanding leg of the lateral bracing angle was coped at the connection to the strut to minimize any in-plane restraint from the lateral bracing. All lateral bracing was approximately 7 feet in length and bolted to rigid structural wall.

3.3 Material Properties

The truss specimens and lateral bracing were fabricated from structural steel conforming to ASTM A36. Representative material samples were obtained to define the mechanical properties of the material for each truss. Eight sheet type tensile coupons conforming to ASTM A 370-77 [1989] were obtained from each truss. One coupon was taken from the flange and one from the web of the tee sections L1-L2 and U1-U2 for each truss. Two coupons were also taken from each leg of an angle in struts U1-L2 and L2-U2.

The coupons were tested in a 120,000 pound capacity Baldwin testing machine. The load rate was maintained at approximately 2000 pounds per minute. During the test, an extensometer was attached to the neck of each coupon and a stress-strain curve was simultaneously plotted. The general shape of these curves, obtained experimentally, are typical for mild steel

01459

[Willems et al. 1981]. A sketch showing a representative stress strain curve and dimensions of the tensile coupons tested is shown in Figure 3.4. The average static yield stress for the sheet-type coupons obtained from the structural tee chord members was 48.8 ksi. The average static yield stress for the sheet-type specimens removed from the double angle web members was 51.6 ksi. Yield stress results for each truss are summarized in Table 3.2.

3.4 Specimen Preparation

After fabrication, the line of action for each member was marked on one side of the truss with a grease pencil so eccentricities could be measured. A theoretical work point for each joint was determined and the eccentricity of each member framing into the joint was measured.

Micro Measurements type EA-06-120LZ-120 linear and type EA-06-060RZ-120 rosette strain gauges were installed at joints U3 and L4 for each truss. Strain gauge locations are shown in figures 3.6a-c. The 120 ohm strain gauges were temperature compensated, polyimide encapsulated, and had a gauge length of 0.120 inch and 0.060 inch for the linear and rosette gauges respectively. The specimen surface at gauge locations was polished using a fine grit sand paper. The surface was then cleaned and gauges installed following the standard procedures outlined by Micro Measurements.

One side of joints L2 and U2 were buffed to remove rust and scale and painted with a thin coat of whitewash. The whitewash acted as a brittle surface coating which cracked and flaked in highly strained regions. Thus, the

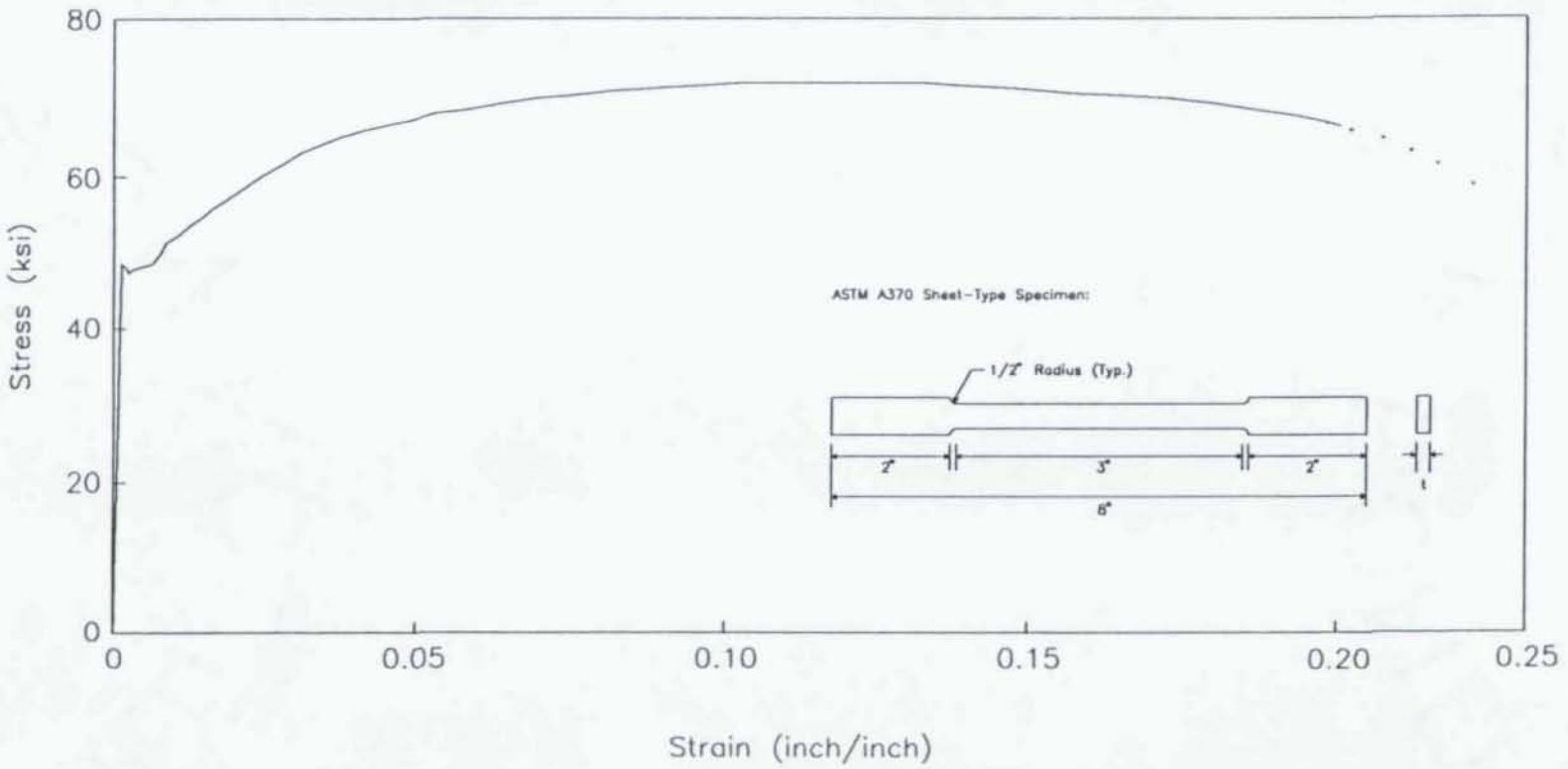


Figure 3.4 Typical Coupon Stress Strain Curve

30

Truss	Tee Section		Angle Section	
	Average Yield Point	Standard Deviation	Average Yield Point	Standard Deviation
#1	48.8 ksi	1.3	49.0 ksi	0.8
#2	48.0 ksi	1.1	50.9 ksi	0.8
#3	48.4 ksi	0.9	53.8 ksi	2.9
#4	49.9 ksi	0.6	52.5 ksi	1.1
#5	49.0 ksi	0.7	52.0 ksi	3.6
Average	48.8 ksi	0.9	51.6 ksi	1.9

Table 3.2 Average Material Yield Stress

01467

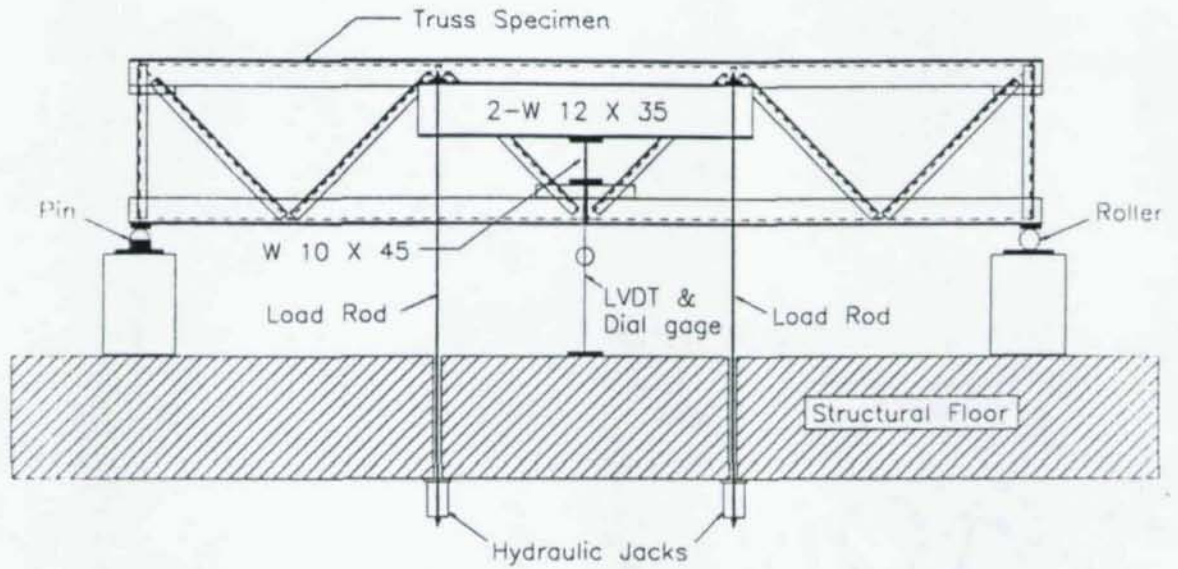
whitewash acted as a visual indicator during the test so that potential problem areas of high strain could be identified within the connection.

3.5 Load System

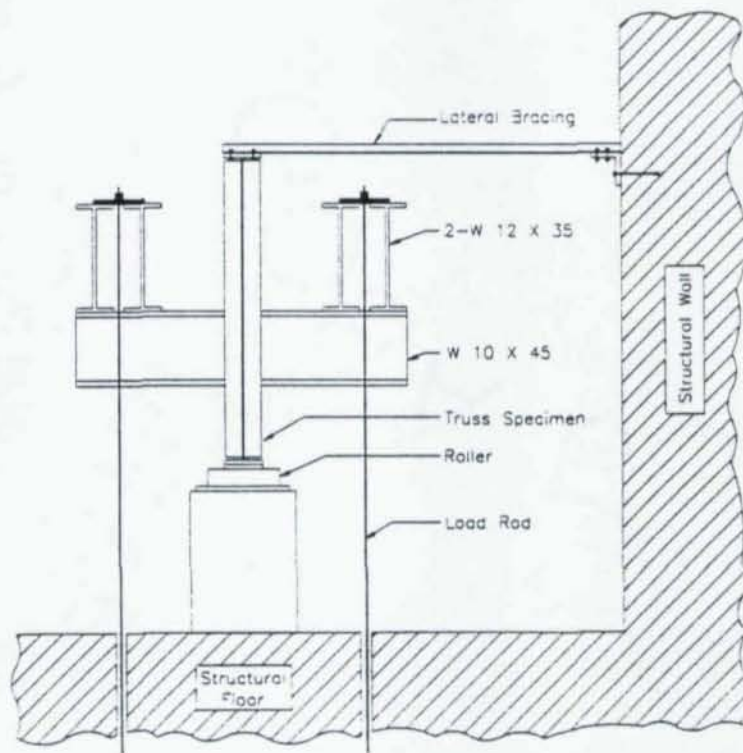
The primary truss loads were applied to the test specimens at joint L3 with the load yoke (Figure 3.5). The single concentrated tension load was selected so equal axial forces were present in each diagonal. Since the design and fabrication of the truss was symmetric, the behavior of joints L2 and U2 were similar to that of joints L4 and U3 respectively.

The test trusses were supported by a steel pin and a roller at joints L1 and L5, respectively. The pin and roller were set on a 15" X 15" X 24" concrete pedestals. The contact surface between the steel and concrete pedestal was leveled by using a high strength gypsum cement.

Loads were applied by four hydraulic jacks located below the structural floor through four 1 inch diameter load rods. The load rods were strain gauged and calibrated as load cells. The load rods transferred the load to two short longitudinal load beams (2-W 12 X 35). The longitudinal load beams rested on a transverse load beam, W 10 X 45 with 5/8 inch cover plates, located at joint L3 (see Figure 3.5). The hydraulic jacks were powered by an Enerpack hydraulic dual stage hand pump. The hydraulic jacks were connected to the hand pump by means of a manifold used to ensure an even distribution of pressure to each jack. The dead weight of the load yoke was 2 kips. This included the weight of the two longitudinal load beams, the transverse load



Side View



End View

Figure 3.5 Loading System

51464

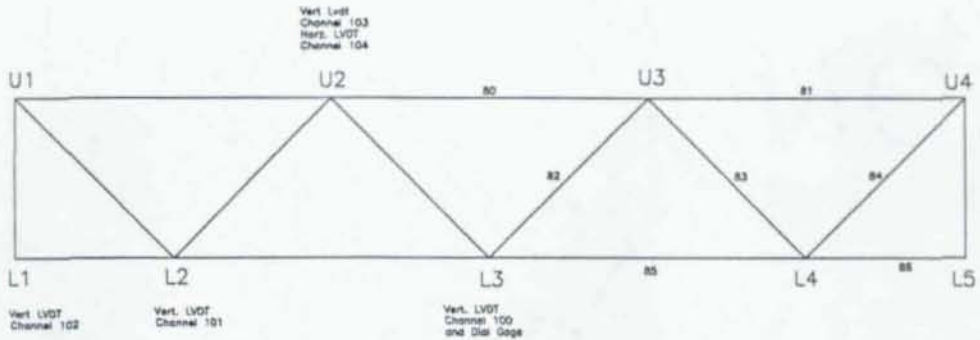
beam, four load rods, four hydraulic jacks, and all bearing plates. This weight was a dead load weight at joint L3 applied to the structure prior to the test and therefore, was added to the applied load measured throughout the test.

3.6 Instrumentation

The strain gauges on the load rods and test specimen were connected to a Hewlett-Packard data acquisition system. Vertical deflections at panel points L1, L2, L3, and U2 were recorded using Linear Voltage Displacement Transducers (LVDT). Strain gauge and LVDT locations for each truss are shown in Figures 3.6a-c. The average dimensions of the cross sections at gauge locations are listed with their corresponding AISC [1989] values in Table 3.3. Typically, both linear and rosette type strain gauges were placed along the center line of the connection. The gauges provided normal strain distributions. These strain distributions were used to calculate axial forces and moments within the joint. The rosette gauges also provided information about the shear strain distribution within the joint. Throughout each test, a continuous plot of applied load versus deflection at joint L3 was made. The data acquisition system recorded the load and displacement voltages and then updated the plot at approximately five second intervals throughout the test.

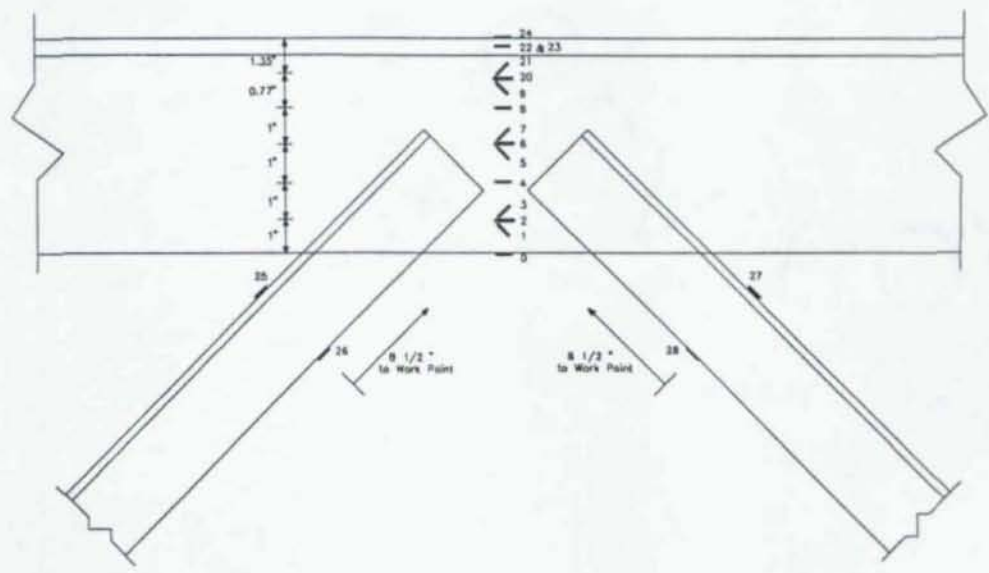
3.7 Test Procedure

The trusses were loaded to 25 kips and then unloaded to ensure proper operation of the data acquisition system. Zero readings for all of the strain



• Gages 80-87 placed on the neutral axis of the section.

Joint U3:



Joint L4:

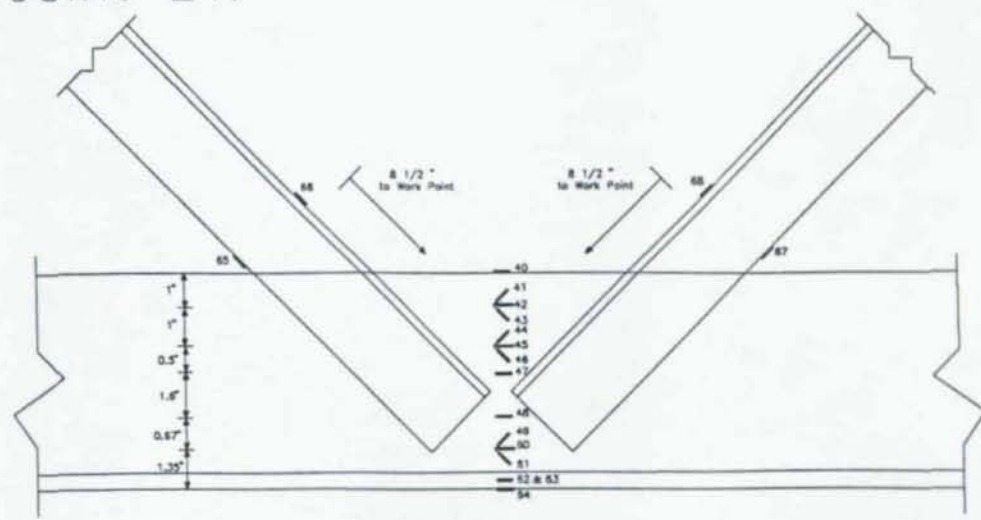
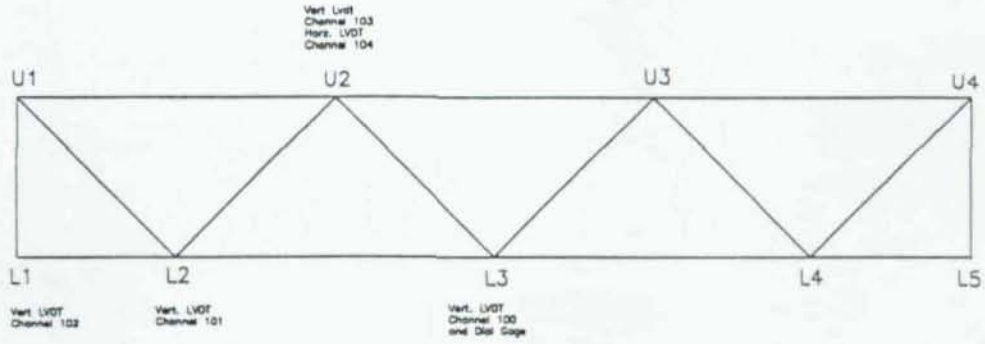
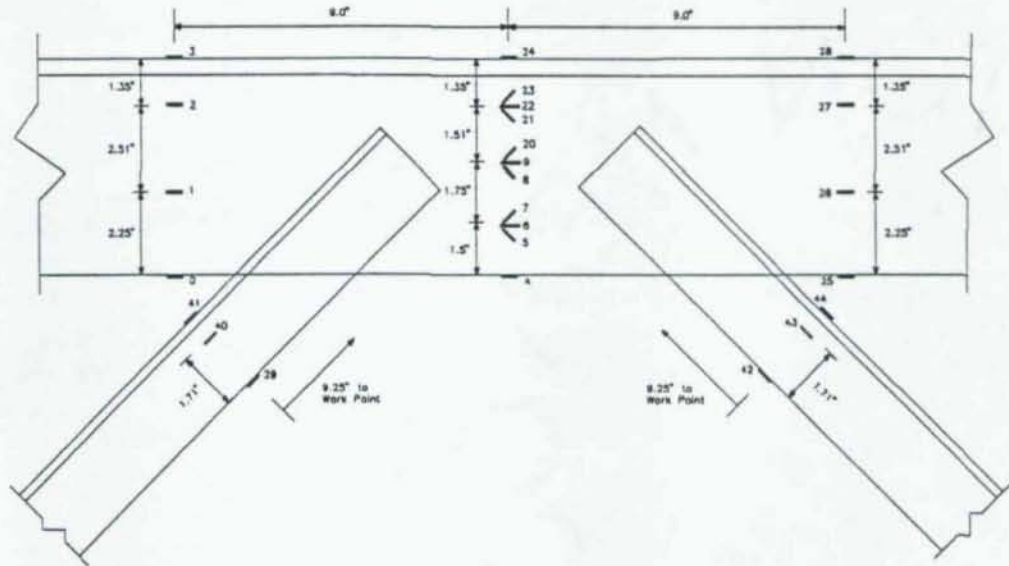


Figure 3.6a Gauge Locations Truss #1



Joint U3:



Joint L4:

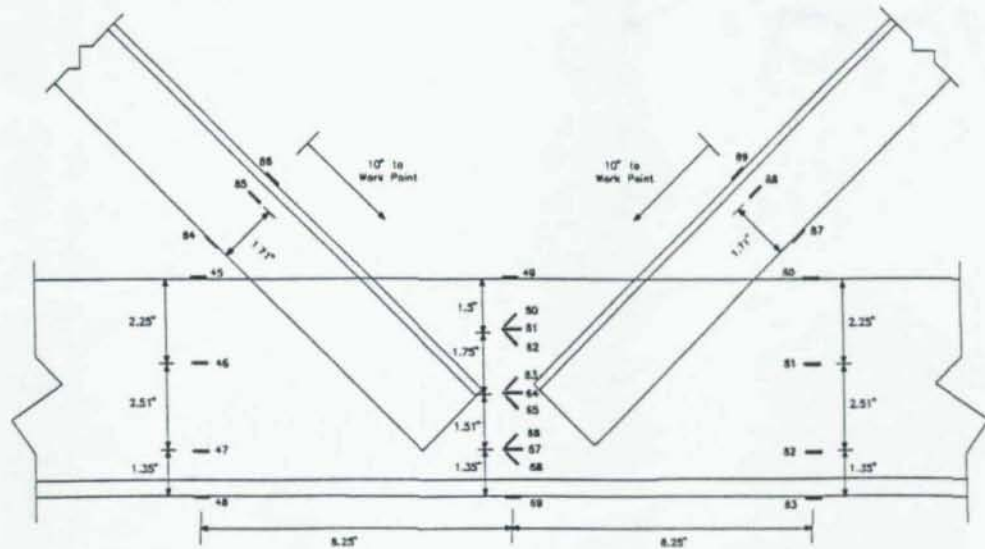
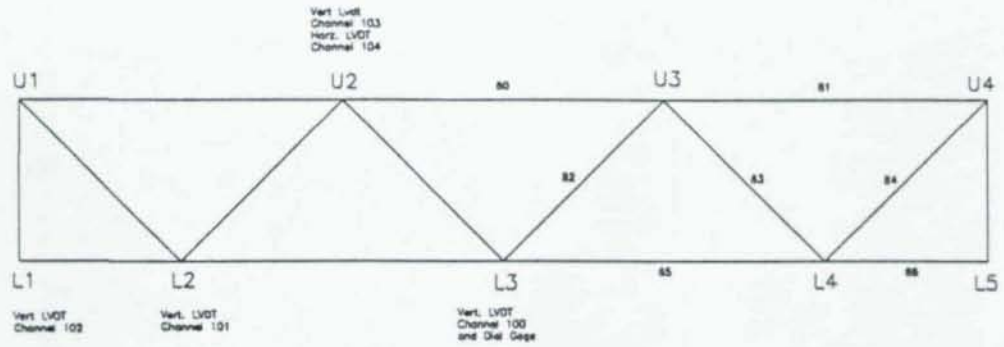
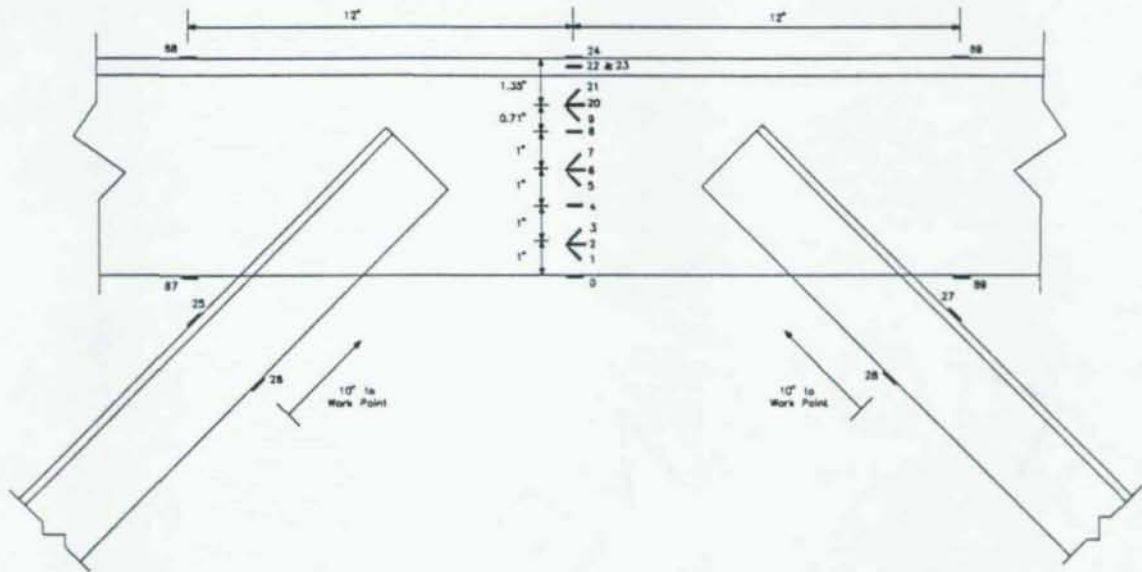


Figure 3.6b Gauge Locations Truss #2, 3, & 5



* Gages 80-86 placed on the neutral axis of the section.

Joint U3:



Joint L4:

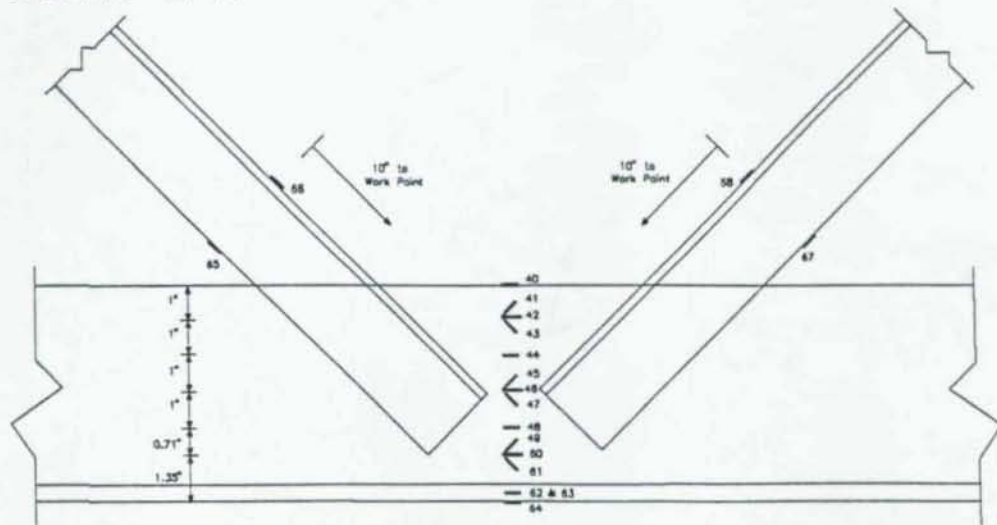
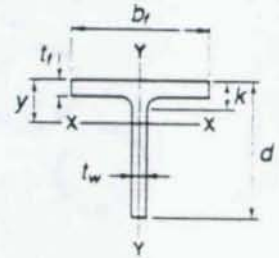


Figure 3.6c Gauge Locations Truss #4

01458

Tee Chord :

	Average Value	AISC Value
d	6.12 in.	6.25 in.
tw	0.33 in.	0.30 in.
bf	6.48 in.	6.56 in.
tf	0.50 in.	0.52 in.
A	5.11 in. ²	5.17 in. ²
y	1.36 in.	1.30 in.
lx	15.9 in. ⁴	16.0 in. ⁴
rx	1.76 in.	1.76 in.
ly	11.4 in. ⁴	12.2 in. ⁴
ry	1.49 in.	1.54 in.



Double Angle Web Members :
(5/16" back to back spacing)

	Average Value	AISC Value
t	0.25 in.	0.25 in.
L1	1.97 in.	2.00 in.
L2	2.48 in.	2.50 in.
A	2.10 in. ²	2.13 in. ²
y	0.783 in.	0.787 in.
lx	1.27 in. ⁴	1.31 in. ⁴
rx	0.778 in.	0.784 in.
ly	0.848 in. ⁴	0.883 in. ⁴
ry	0.635 in.	0.648 in.

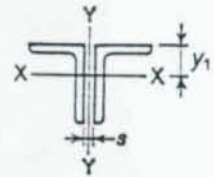


Table 3.3 Cross-Section Dimensions and Geometric Properties

gauges and LVDTs were recorded. In general, the load was applied in increments of 10 kips until the overall response of the truss became non-linear. After the first sign of non-linearity, the load increments were reduced to approximately 5 kips until the truss no longer carried additional load. The mid-span deflection was constantly monitored with a 2½ inch Enco dial gauge and a LVDT. Strain gauge and LVDT readings were then recorded while the applied load was kept constant.

Photographs of the truss were taken before and after each test. The time required for one test was about 45 minutes. After failure, the truss was flame cut and tensile coupons were machined from the members well away from heat affected zones.

Chapter 4

Experimental and Analytical Results

4.1 Truss Specimen Behavior

Failure of all five trusses occurred in the compression chord U2-U3. However, since each truss had different eccentricities, several truss specimens had different characteristics at failure. As each of the five trusses reached its ultimate capacity, the top chord member U2-U3 buckled. The deflection of member U2-U3 was *in-plane* for all five truss specimens with no noticeable out-of-plane or twisting displacement until the peak load was reached. As the peak load was reached, out-of-plane and torsional displacement of chord member U2-U3 occurred. After the ultimate capacity was reached, hydraulic fluid displacement to the load system was continued; the ultimate load resisted by the structure was maintained while the structure continued to deflect. It is at this point during testing that the failure characteristics began to differ. The continued application of hydraulic pressure caused further deflection of the structure and each truss deteriorated due to lateral-torsional buckling of compression member U2-U3 (Figure 4.1). In addition, truss #3's compression strut L2-U2, between joint L2 and the mid-length fastener of the strut, buckled as deflection of the structure continued to be induced (Figure 4.1c). As deflection of truss #4 continued to be induced, local buckling of the stem of the



Figure 4.1 a Failure Truss #1

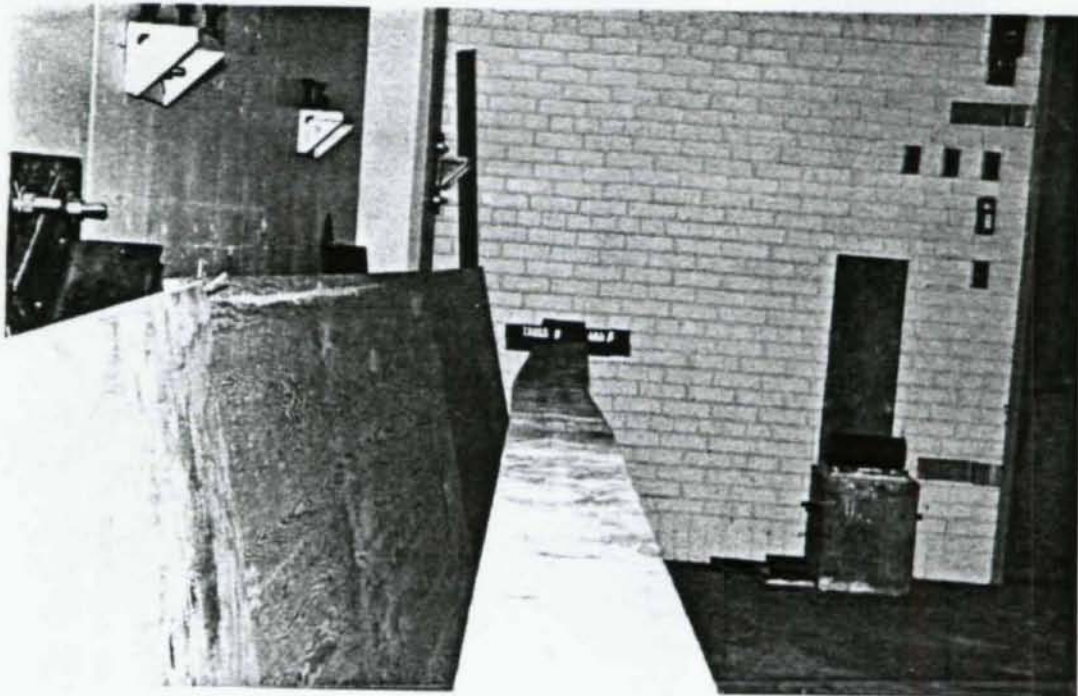


Figure 4.1 b Failure Truss #2

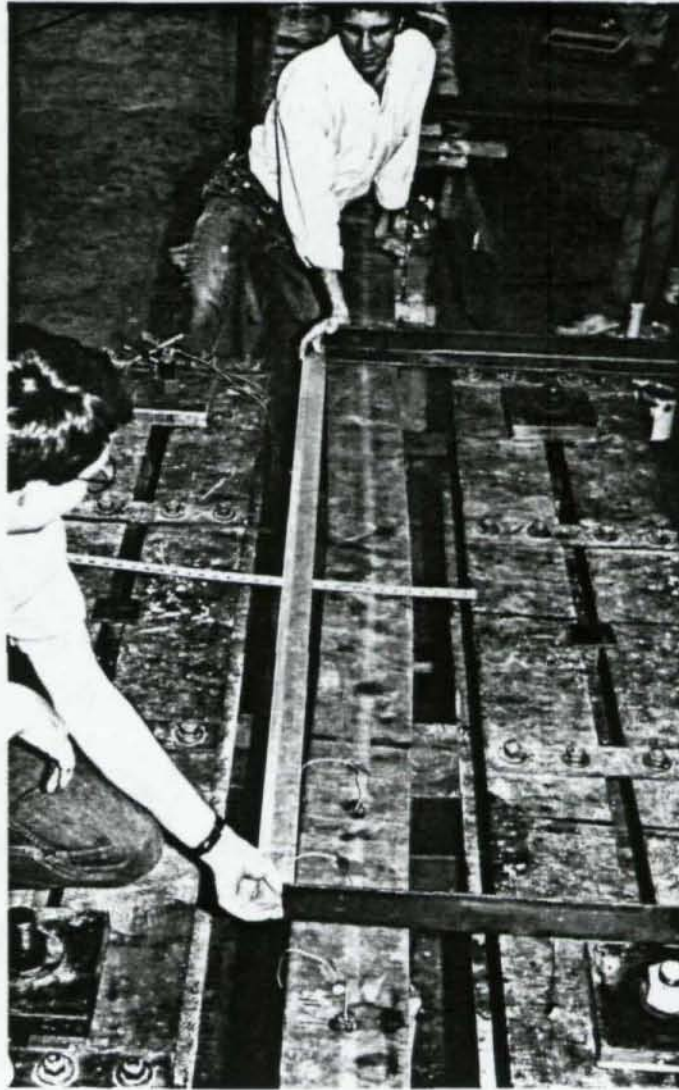


Figure 4.1 c Failure Truss #3

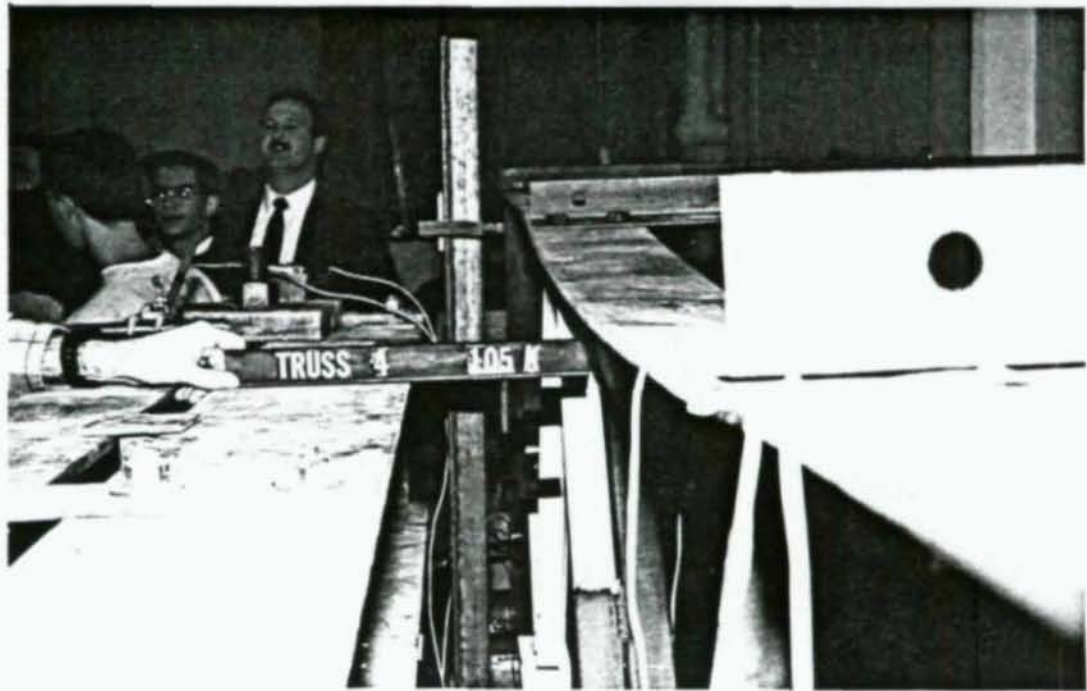
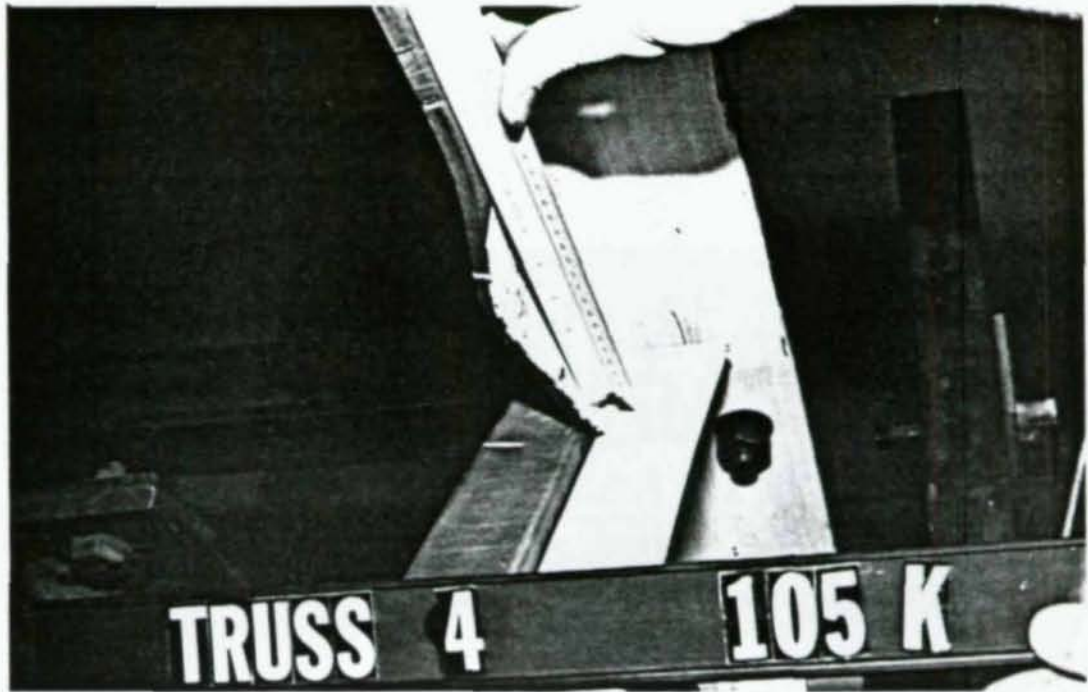


Figure 4.1 d Failure Truss #4

01475
structural tee chord U1-U2 just outside of joint U2 occurred (Figure 4.1d).

As the trusses were subjected to increasing loads, some flaking and cracking of the whitewash at joints L2 and U2 was observed. The cracking and flaking appeared to start at lighter loads within the concentric or nearly concentric connections as compared with the eccentric connections.

Whitewash flaking typically occurred along the weld at the heel and/or toe of the angle web members. Flaking of the whitewash tended to be more severe between the tips of the web members closest together.

The effects of in-plane bending moments and continuity of the chord were evident, as reverse curvature of the top compression chord was observed prior to failure. As would be expected, the greater the top chord eccentricity, the more pronounced the reverse curvature displacements.

A continuous plot of applied load versus deflection at joint L3 was made during each test. The plot from each of the five trusses tested has been reproduced in Figure 4.2. As can be seen from Figure 4.2, truss #1 with eccentricities less than or equal to 1/4 inch (the nearly "perfect" truss), was the stiffest structure of the five specimens tested and had an ultimate carrying capacity of 140 kips. As positive joint eccentricities are introduced, the structure response becomes softer. Truss #3, with approximately a two inch positive eccentricity at joints L2 and L4 on the tension chord, was a "softer" structure than the "nearly perfect" truss but had an identical peak load of 140 kips. Truss #2 however, with approximately a two inch positive eccentricity at joints U2 and U3 on the compression chord, appeared to be slightly stiffer than

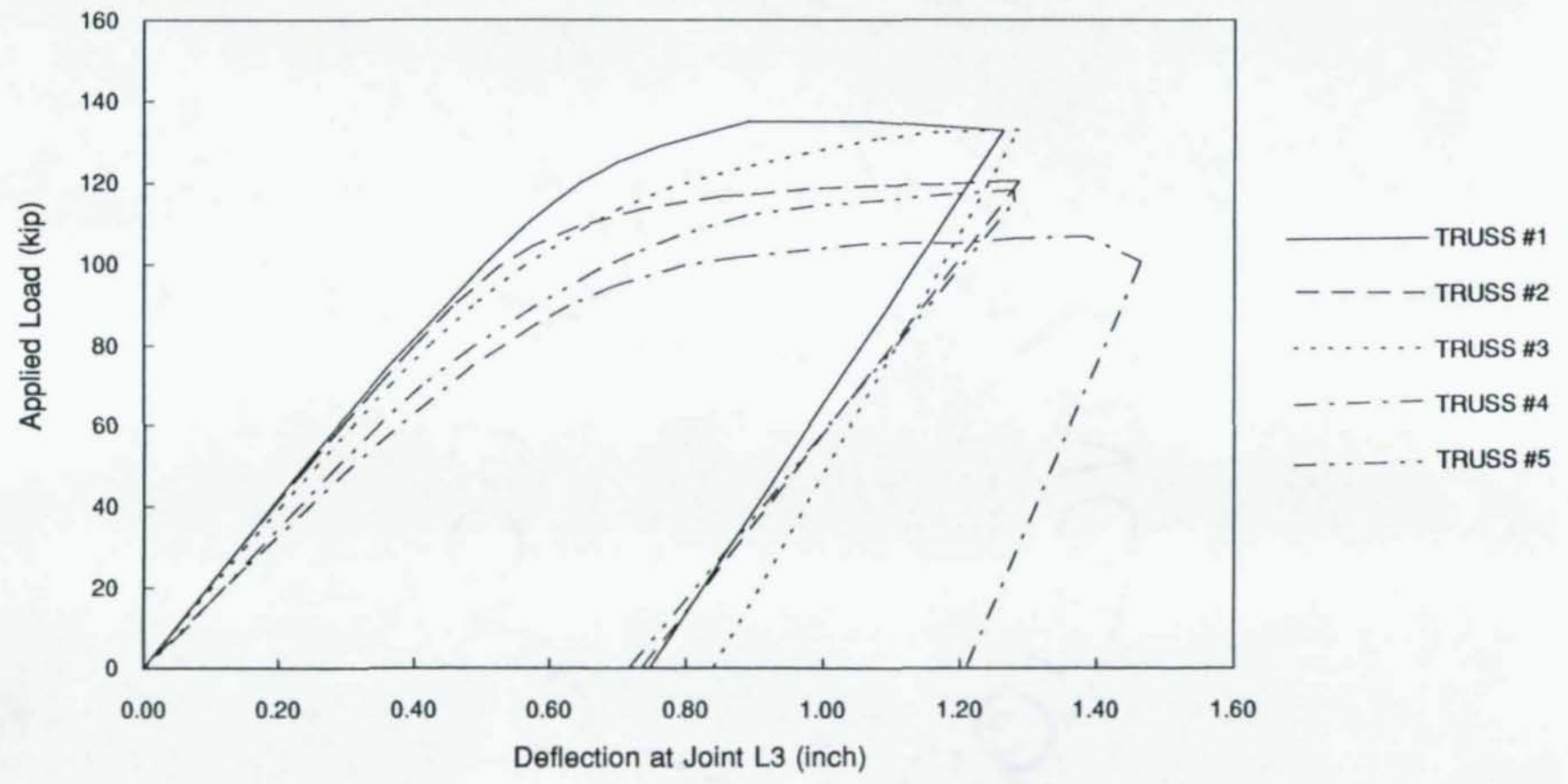


Figure 4.2 Applied Load vs. Deflection Curves

91477

truss #3 until just before failure, although truss #2 had a 12.8% reduction of peak load when compared with trusses #1 and #3, resisting 122 kips.

As expected, the truss structure lost stiffness and load carrying capacity as the magnitude of the eccentricity was increased. Truss #4, with approximately a four inch eccentricity on the compression chord and a one inch eccentricity on the tension chord and truss #5 with approximately a four inch eccentricity on the tension chord and a one inch eccentricity on the compression chord were less stiff than the three truss specimens with lesser eccentricities. Truss #4 failed at an ultimate load of 110 kips where truss #5 failed at 121 kips.

These effects of top chord eccentricity verses ultimate load are shown in Figure 4.3. The capacity of a truss specimen with eccentricities present only in the top chord joints was predicted using a plane frame analysis, assuming linear elastic material, and is plotted in figure 4.3. Large positive eccentricities on the bottom chord have a small influence on the ultimate capacity of the truss specimens. Truss #3, with nearly perfect top chord joints and approximately two inch eccentricities at joints L2 and L4, had the same carrying capacity as truss #1, the nearly perfect truss. Truss #5 with approximately one inch eccentricities at joints U2 and U3 and four inch eccentricities at joints L2 and L4 fell below the best fit line of the trusses with primary eccentricities on the top chord, by approximately 9 kips.

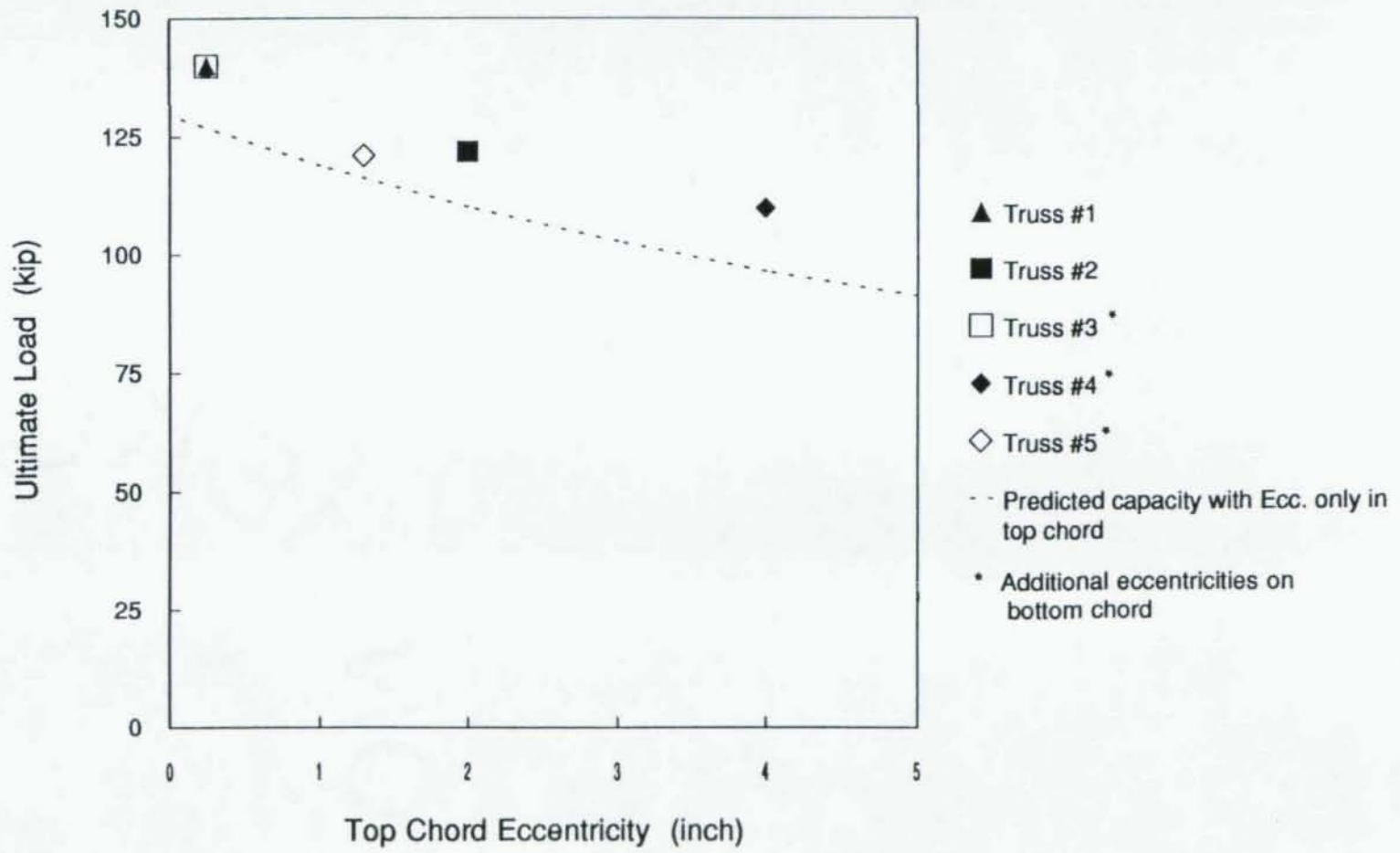


Figure 4.3 Ultimate Load vs. Top Chord Eccentricity

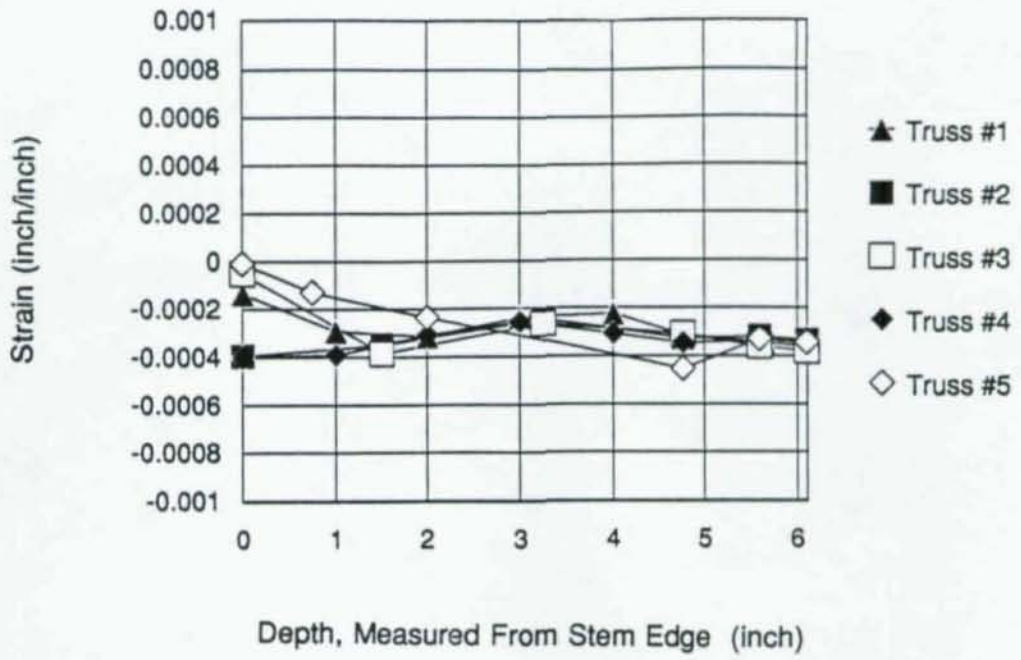
4.2 Analysis of Member End Forces

4.2.1 Experimental Determination of Member End Forces

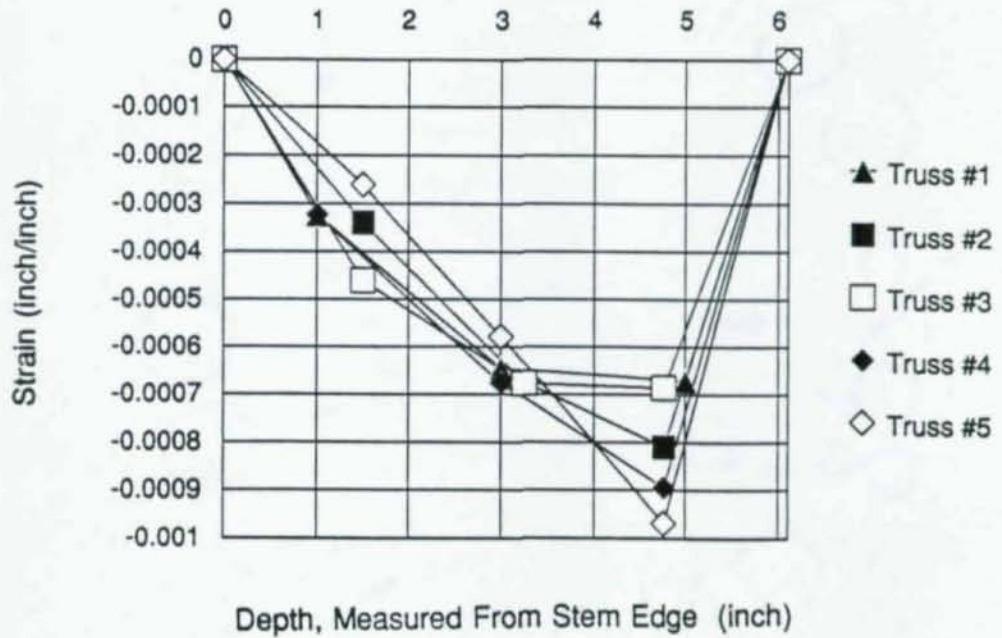
Readings from strain gauges placed at joints U3 and L4 have been utilized to provide information not only about generalized strain distributions at the connection locations but also axial, shear, and moment forces at the connections. Typical curves of normal and shear strain distributions along the center line of the connections and normal strain distributions for members adjoining the connections at an applied load of 50 kips are shown in Figures 4.4 a, b, e, & f. An applied load of 50 kips was selected because it was the design load for the structure and was still within the elastic range of the loading spectrum.

The strain distributions were generated based on the assumption that there was a linear strain relationship between gauges. As can be seen from Figure 4.4 a-d, there are no significant discontinuities of the normal strain distributions at joint U3. There are, however, significant strain gradients shown within the stem of the normal strain distributions at joint L4 (Figure 4.4 f), suggesting that the stem of the tee carries the bulk of the load while the flange contributes very little. This is as expected as member L4-L5 theoretically carries no load and thus, all forces from member L3-L4 must be reacted by the web members connected to the stem of the tee chord. The shear strain distributions at joints U3 and L4 were similar to that of the expected parabolic distribution along the depth of the tee stem.

A stress distribution can be determined from each strain distribution

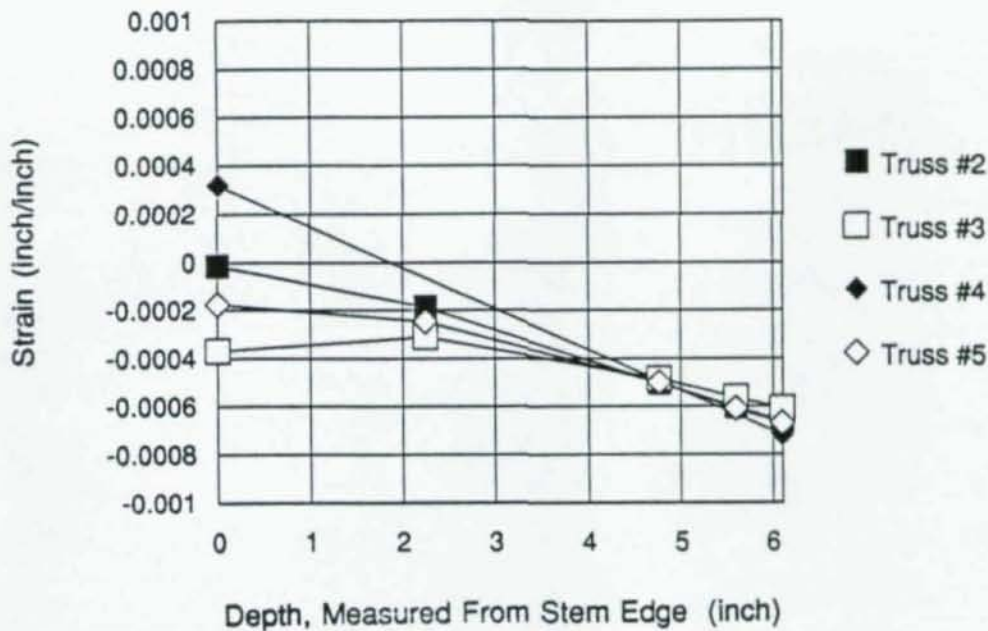


(a) Normal Strain Distribution Center-Line Joint U3

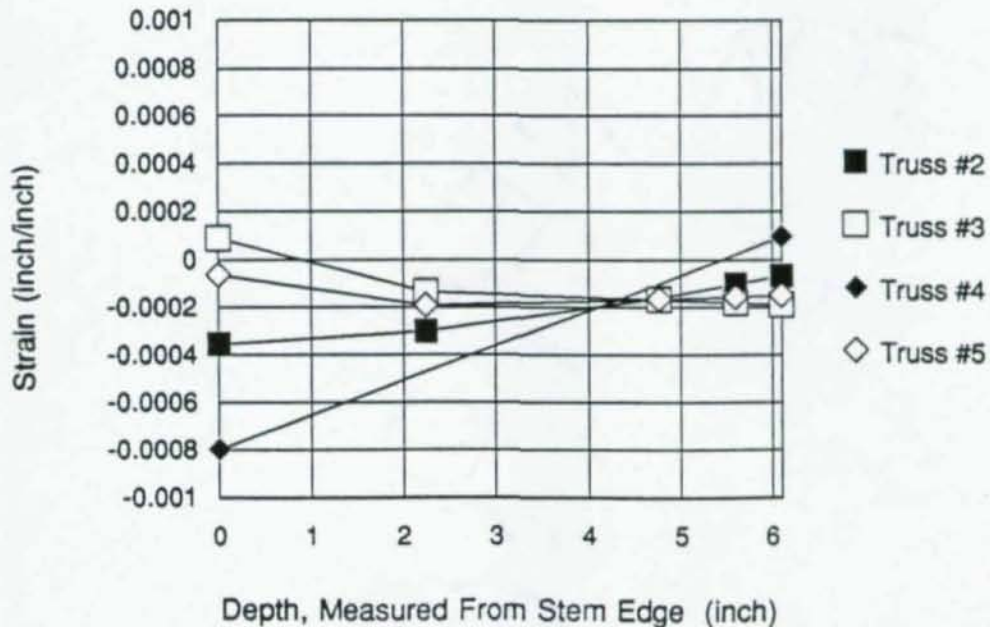


(b) Shear Strain Distributions Center-Line Joint U3

Figure 4.4 a & b Strain Distributions at P = 50 Kips

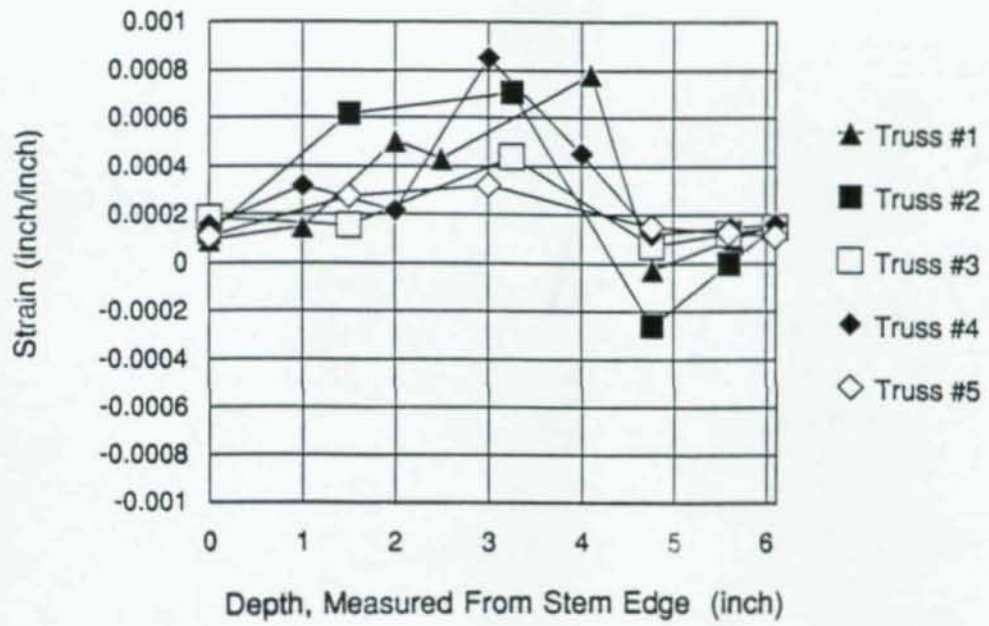


(c) Normal Strain Distributions Member U2-U3 at Joint U3

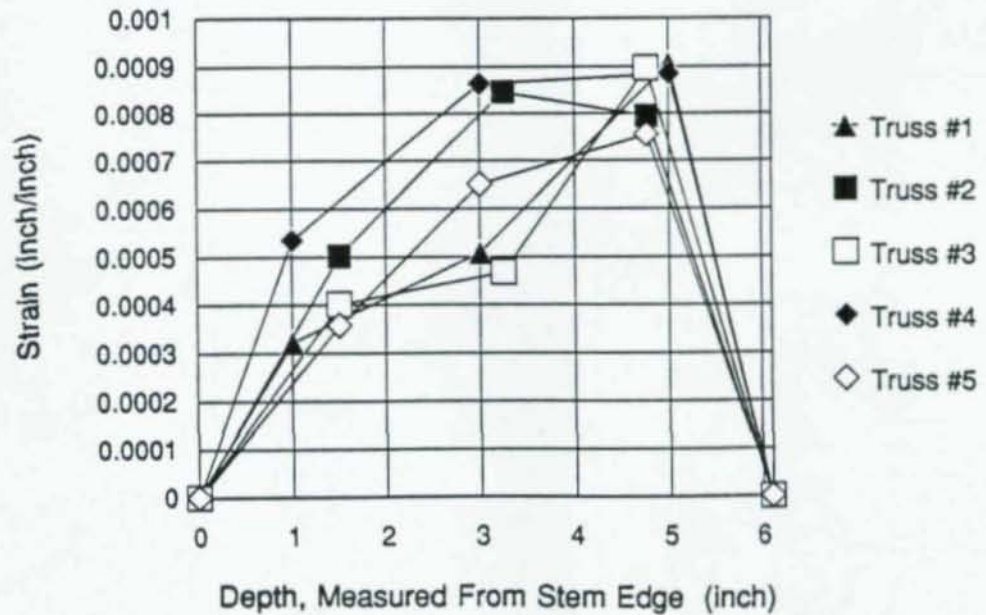


(d) Normal Strain Distributions Member U3-U4 at Joint U3

Figure 4.4 c & d Strain Distributions at P = 50 Kips

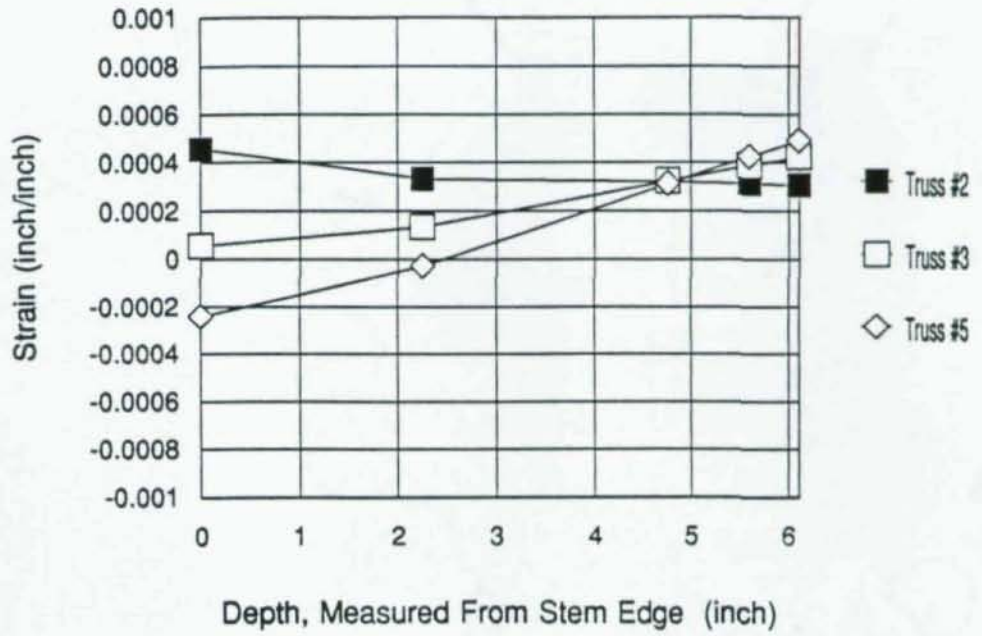


(e) Normal Strain Distributions Center-Line Joint L4

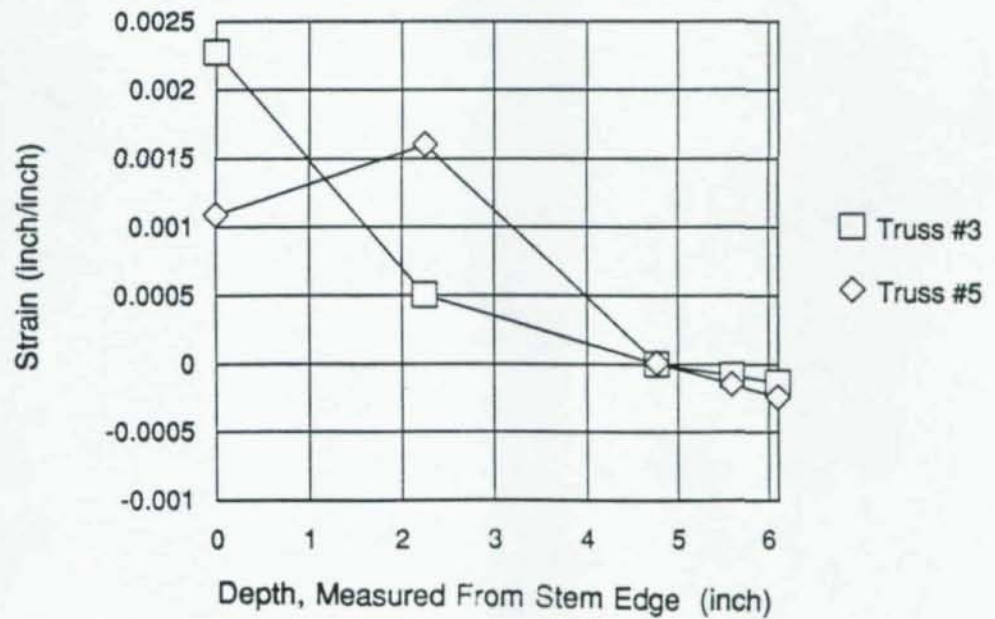


(f) Shear Strain Distributions Center-Line Joint L4

Figure 4.4 e & f Strain Distributions at P = 50 Kips



(g) Normal Strain Distributions Member L3-L4 at Joint L4



(h) Normal Strain Distributions Member L4-L5 at Joint L4

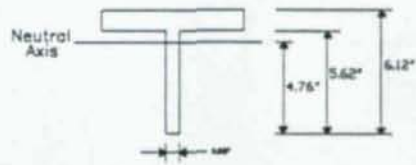
Figure 4.4 g & h Strain Distributions at P = 50 Kips

based on the material's properties. The material was assumed to be elastic perfectly plastic with a yield stress equal to 48.8 ksi. Elastic beam theory is based on the assumption that plane sections normal to the axis of a beam remain plane after bending, thus producing a linear strain distribution across the cross-section. Naturally, a pure axial force would produce a uniformly linear strain distribution across the section. These assumptions have been shown experimentally to be very good even when extended into the plastic range [Timoshenko 1966] and are incorporated into the basic assumptions used in the following analysis.

Stress and strain are directly proportional for stresses below the proportional limit. When stresses exceed the proportional limit, this is no longer applicable, but the linear distribution of strain is assumed to remain valid. Thus, the stress corresponding to the strains above the proportional limit must be determined from the properties of the material.

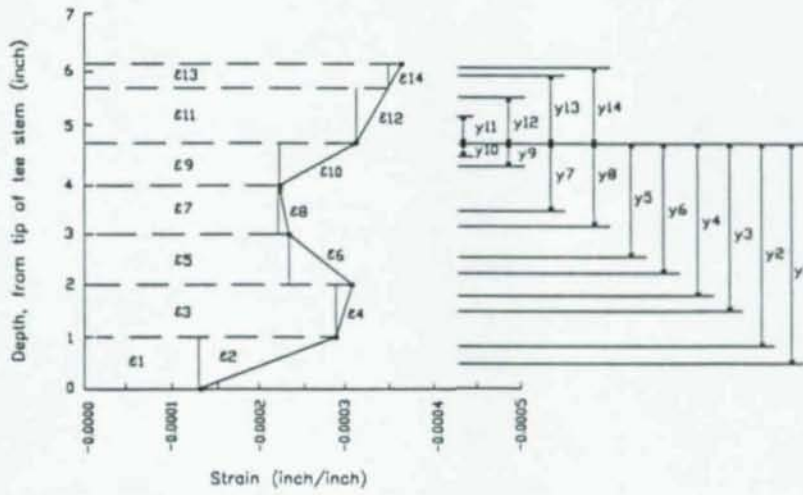
Member forces at gauged cross-sections can be determined from the strain distributions (Figure 4.5). The experimentally determined normal strain distributions are a summation of axial and bending forces on the section. Since the net axial resultant of the bending portion of the combined strain diagram is zero, the axial force is a product of the area under the strain curve, ϵ_i , Young's modulus, E , and the cross-sectional area on which the strain is acting, A_i (ie. $P = \sum(\epsilon_i * E * A_i)$).

The bending moment about a point on the cross-section, typically the centroidal axis, can similarly be determined (Figure 4.5). First calculate the



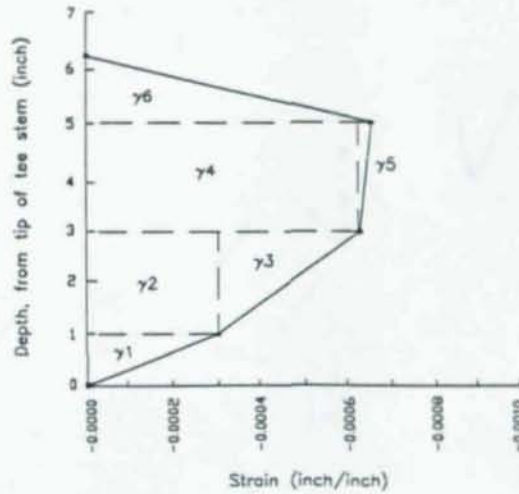
Gaged Cross-Section

(a)



Typical Normal Strain Distribution

(b)



Typical Shear Strain Distribution

(c)

Figure 4.5 Typical Strain Distributions for Member Force Calculations

area under the strain curve above and below the point of interest. Then calculate the distance (moment arm) from the point of interest to each area's respective centroid. The moment is the product of each area under the strain curve, ϵ_i , Young's modulus, E , the respective moment arm, y_i , and cross-sectional area upon which they act, A_i (ie. $M = \sum (\epsilon_i * E * A_i * y_i)$).

The shear forces were calculated assuming only the web material resists shear, and the contribution of the flange is negligible. This assumption has been shown to be experimentally and theoretically valid for sections with relatively thin flanges [Salmon 1980]. The shear force is the product of the area under the shear strain curve, γ_i , shear modulus, G , and the cross sectional area of the web material upon which it acts, $d_i * t_{wi}$, (ie. $V = \sum (\gamma_i * G * d_i * t_{wi})$). The shear strains were not directly measured along the stem of the tee. Strain rosettes were used to measure the strain in three directions about a point. The strain rosettes were placed such that the angle θ measured from the longitudinal axis of the member was 45 degrees. The shear strain was calculated using the following strain transformation equations [Measurements 1990]:

$$\frac{\gamma_{xy}}{2} = -\frac{\epsilon_x - \epsilon_y}{2} \sin 2\theta + \frac{\gamma_{xy}}{2} \cos 2\theta \quad (4.1)$$

where

$$\gamma_{xy} = 2\epsilon_b - \epsilon_a - \epsilon_c$$

In the case of a double symmetric section, the point of zero stress (neutral axis) due to bending coincides with the axis of symmetry (centroidal

axis) about which the section is being bent. However, the point of zero stress due to bending shifts from the centroidal axis for the case of a singly symmetric section. Thus, for consistency, all member moments in this report are taken about the members centroidal axis and not necessarily their axis of zero bending stress. Therefore, analytical results from a standard plane frame analysis and experimental values may be directly compared.

4.2.2 Theoretical Determination of Member Forces

A plane truss, consisting of two degree of freedom elements which only considers axial forces, is typically used for the analysis of most planar trusses. Stresses due to the stiffness of the connection and continuity of the chords are considered secondary and are neglected in such an analysis. However, when joint eccentricity is introduced, an element considering axial, shear, and moment forces must be used to account for the induced stresses. Therefore, member force values for the truss specimens were estimated with IMAGES-3D Finite Element Analysis Program, using a standard six degree of freedom plane frame element, considering axial, shear, and moment forces [Celestial Software 1988]. The chords were modeled as continuous members with nodes for web members at the location of actual intersection points of the members centroidal axes, not necessarily the theoretical work point for the joint.

High shear forces are typically found in truss connections as web members transfer their loads through the stem of the tee chord. If the connection is concentric, then theoretically no moments are introduced within

01488

the connection due to the shear load transfer. However, a connection with a significant positive eccentricity behaves much like a short beam with high shear loads and consequently high moments. Because the top chord is continuous and the connections are rigid, moments due to joint eccentricity within the connection significantly affect the members framing into the connection.

4.2.3 Comparison of Experimental and Analytical Member End Forces

A summary of the experimentally determined member forces at joints U3 and L4 and their corresponding analytically determined values at the design load of 50 kips are presented in Tables 4.1a-e. The experimentally determined values were calculated using the actual dimensions and properties of the cross section, while the analytically determined values were calculated using the AISC assumed dimension values (see Table 3.3).

The axial forces calculated at the center line of the structural tee chord within joints U3 and L4 obtained from the normal strain distributions are within ± 14 percent of those obtained using the plane frame model. The axial member forces determined from strain distributions measured in the critical member U2-U3 are within 3 percent of those obtained analytically using the plane frame model.

Based on analytical and experimental results, the presence of positive eccentricities of two inches and four inches on the top or bottom chord appear to have had a negligible influence on the magnitude of the axial member forces.

The member end moments are approximately proportional to the

Location		Truss #1		
		Experimental	Analytical	% Difference
Center Line Joint U3	Axial	-47.4	-48.8	-2.9
	Moment	11.1	19.1	-41.9
	Shear	20.4	24.4	-16.4
Member U2-U3	Axial Moment	****	****	****
Member U3-U4	Axial Moment	****	****	****
Center Line Joint L4	Axial	28.1	25.0	12.4
	Moment	-19.1	-1.9	905.3
	Shear	21.2	23.3	-9.0
Member L3-L4	Axial Moment	****	****	****
Member L4-L5	Axial Moment	****	****	****

*** Not Available

Table 4.1a Member Forces Truss #1

Location		Truss #2		
		Experimental	Analytical	% Difference
Center Line Joint U3	Axial	-47.6	-49.2	-3.3
	Moment	13.3	11.8	12.7
	Shear	20.9	24.4	-14.3
Member U2-U3	Axial	-74.1	-72.3	2.5
	Moment	51.8	53.4	-3.0
Member U3-U4	Axial	-21.3	-25.4	-16.1
	Moment	-25.8	-30.6	-15.7
Center Line Joint L4	Axial	23.8	25.4	-6.3
	Moment	30.7	-5.4	-668.5
	Shear	24.8	25.4	-2.4
Member L3-L4	Axial	48.0	49.1	-2.2
	Moment	3.5	3.1	12.9
Member L4-L5	Axial	****	****	****
	Moment			

*** Not Available

Table 4.1b Member Forces Truss #2

Location		Truss #3		
		Experimental	Analytical	% Difference
Center Line Joint U3	Axial	-49.7	-48.7	2.1
	Moment	11.2	19.9	-43.7
	Shear	21.0	25.2	-16.7
Member U2-U3	Axial	-75.8	-73.6	3.0
	Moment	27.5	27.6	-0.4
Member U3-U4	Axial	-22.6	-25.1	-10.0
	Moment	16.9	15.9	6.3
Center Line Joint L4	Axial	23.3	25.1	-7.2
	Moment	6.6	5.7	15.8
	Shear	20.1	24.6	-18.3
Member L3-L4	Axial	48.3	48.7	-0.8
	Moment	-32.0	-33.7	-5.0
Member L4-L5	Axial	2.8	0.8	250.0
	Moment	36.6	46.5	-21.3

Table 4.1c Member Forces Truss #3

		Truss #4		
Location		Experimental	Analytical	% Difference
Center Line Joint U3	Axial	-51.0	-49.2	3.7
	Moment	5.3	5.7	-7.0
	Shear	23.2	24.3	-4.5
Member U2-U3	Axial	71.6	71.3	0.4
	Moment	79.4	87.0	-8.7
Member U3-U4	Axial	****	****	****
	Moment			
Center Line Joint L4	Axial	28.2	25.1	12.4
	Moment	22.3	9.7	129.9
	Shear	28.1	24.6	14.2
Member L3-L4	Axial	****	****	****
	Moment			
Member L4-L5	Axial	****	****	****
	Moment			

*** Not Available

Table 4.1d Member Forces Truss #4

Location		Truss #5		
		Experimental	Analytical	% Difference
Center Line Joint U3	Axial	-46.3	-48.6	-4.7
	Moment	14.7	17.6	-16.5
	Shear	21.1	25.9	-18.5
Member U2-U3	Axial	-77.6	-73.6	5.4
	Moment	41.6	43.7	-4.8
Member U3-U4	Axial	-22.3	-25.5	-12.5
	Moment	1.9	2.0	-4.0
Center Line Joint L4	Axial	21.9	25.5	-14.1
	Moment	8.0	12.7	-37.0
	Shear	20.6	24.5	-15.9
Member L3-L4	Axial	46.3	48.6	-4.7
	Moment	-67.0	-68.3	-1.9
Member L4-L5	Axial	1.3	0.8	61.3
	Moment	91.1	98.0	-7.0

Table 4.1e Member Forces Truss #5

91494

magnitude of the eccentricity, while, as mentioned previously, the axial forces are essentially insensitive to eccentricity. Large percent differences between experimentally measured and analytical values typically occurred within concentric connections. However, as would be expected, concentric connections had relatively low moments along their center line. Therefore, a large percent difference between experimental and analytical values could exist with a negligible difference of magnitude.

The web members connected to the stem of the tee chord in a concentric joint are typically much closer to the center line of the joint and closer to the bottom of the tee stem than those connected in a positive eccentric joint, to allow the members to align properly. Therefore, it would seem logical that much of the load transferred between the web members within a concentric connection occurs in the lower region of the tee stem and shifted away from the centroidal axis where it is assumed to act. Thus, the strain distribution along the center line of a concentric connection will see a more severe strain concentration in the tee stem between the closely placed members than an eccentric connection. The positive eccentric connections have a larger distance between the web members and the center line of the connection. St. Venant's principle would suggest that the center line of the eccentric connection will see less of the localized effects than the concentric connection.

The shear forces measured along the center line of joints U3 and L4 ranged from -18.5 to 14.2 percent different than those predicted by the plane

frame model. The discrepancy between the theoretical and experimental forces may be the result of: (1) only three rosette gauges were used across the entire tee stem. Thus leaving relatively large gaps between gauge locations and increasing the susceptibility to error due to high strain gradients; (2) the type of rosette strain gauge used can err in regions of high strain gradients. Planar rosettes were used and the individual gauge elements in a planar rosette may sense different strain fields and magnitudes.

4.3 Ultimate Load Capacity Comparisons

The experimentally measured ultimate load capacity for each truss is compared with theoretical ultimate load values and the allowable design load in Table 4.2. Theoretical ultimate load values were determined using the ASD [AISC 1989] and LRFD [AISC 1986] methods, and allowable design loads were determined with the ASD method using the material's actual yield stress of 48.8 ksi and the material's minimum specified yield stress of 36.0 ksi.

Axial-moment interaction in member U2-U3 was the cause of the primary mode of failure for each of the five trusses. Experimental member end forces throughout the loading spectrum were determined from strain distributions as outlined in section 4.2.1. As positive eccentricities were introduced into the frame system, axial member forces remained relatively constant while member moments significantly increased (see M/P ratios, Table 4.2). Axial-moment interaction diagrams for the failed member U2-U3 are shown in Figures 4.6 a-e. The predicted interaction path for each truss was determined using an elastic

Truss	Experimental		Ultimate State				Fy = 48.8 ksi		Fy = 36.0 ksi		M / P Ratio ****
	Applied Load	Failure mode	ASD Analytic*		LRFD Analytic**		ASD Allowable Design Load	Factor of Safety ***	ASD Allowable Design Load	Factor of Safety ***	
			Applied Load	Difference	Applied Load	Difference					
#1	140 kip	T-F Buckling member U2-U3	124 kip	11.4%	119 kip	15.0%	68.4 kip	2.05	53.6 kip	2.61	0.398
#2	122 kip	T-F Buckling member U2-U3	107 kip	10.8%	105 kip	13.9%	59.5 kip	2.05	46.8 kip	2.61	0.830
#3	140 kip	T-F Buckling member U2-U3	125 kip	10.7%	120 kip	14.3%	68.5 kip	2.04	53.7 kip	2.61	0.375
#4	110 kip	T-F Buckling member U2-U3	95 kip	13.6%	94 kip	14.5%	52.8 kip	2.08	41.5 kip	2.65	1.312
#5	121 kip	T-F Buckling member U2-U3	114 kip	5.8%	112	7.4%	63.2 kip	1.91	49.6 kip	2.44	0.594
Perfect Frame		T-F Buckling member U2-U3	130 kip		111 kip		71.4 kip		55.9 kip		0.286
Perfect Truss		T-F Buckling member U2-U3	148 kip		138 kip		80.5 kip		62.3 kip		

* Based on Fy = 48.8 ksi, K = 0.85, a plane frame analysis, and ASD equations with no factor of safety

** Based on Fy = 48.8 ksi, K = 0.85, a plane frame analysis, and LRFD equations with no load or resistance factors

*** Factor of safety; Experimental applied load divided by the allowable design load

**** Moment to axial load ratio for the failed member U2-U3, determined using an elastic plane frame analysis

Table 4.2 Experimental and Theoretical Ultimate Load Capacity

plane frame model.

A general method, based on research by Korol et al. [1986], for predicting the behavior of trusses, was used to predict the ultimate behavior and capacity of the five truss specimens tested. However, the series of load steps and subsequent modification of the structure stiffness for this method, was not necessary because the truss specimens were statically determinate. Failure envelopes with a plot of member forces throughout the loading of each truss for member U2-U3 are presented in Figures 4.6. As can be seen from Figures 4.6, moment unloading of the failing section does typically occur at the time of failure as predicted by the Korol model.

The inner envelope in Figures 4.6 a-e is the AISC [1989] allowable stress design curve for the WT chord, and the outer envelope is the failure curve. The ASD design curve is based on the combined stresses equations:

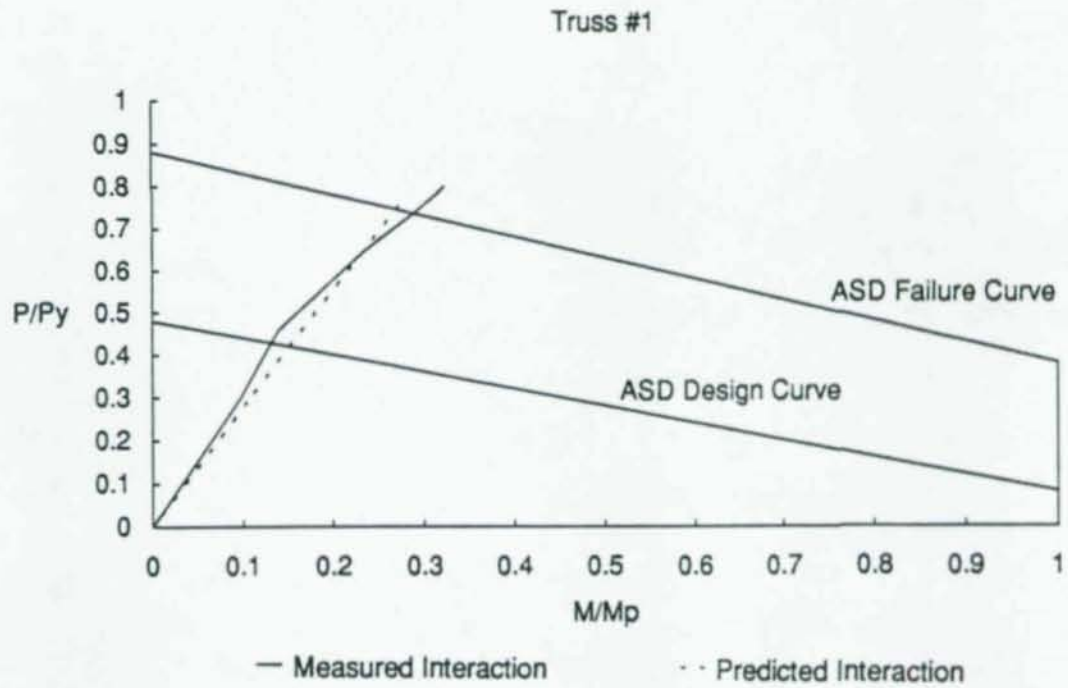
$$\frac{f_a}{F_a} + \frac{C_m f_b}{\left(1 - \frac{f_a}{F_a}\right) F_b} \leq 1.0 \quad (4.2)$$

and

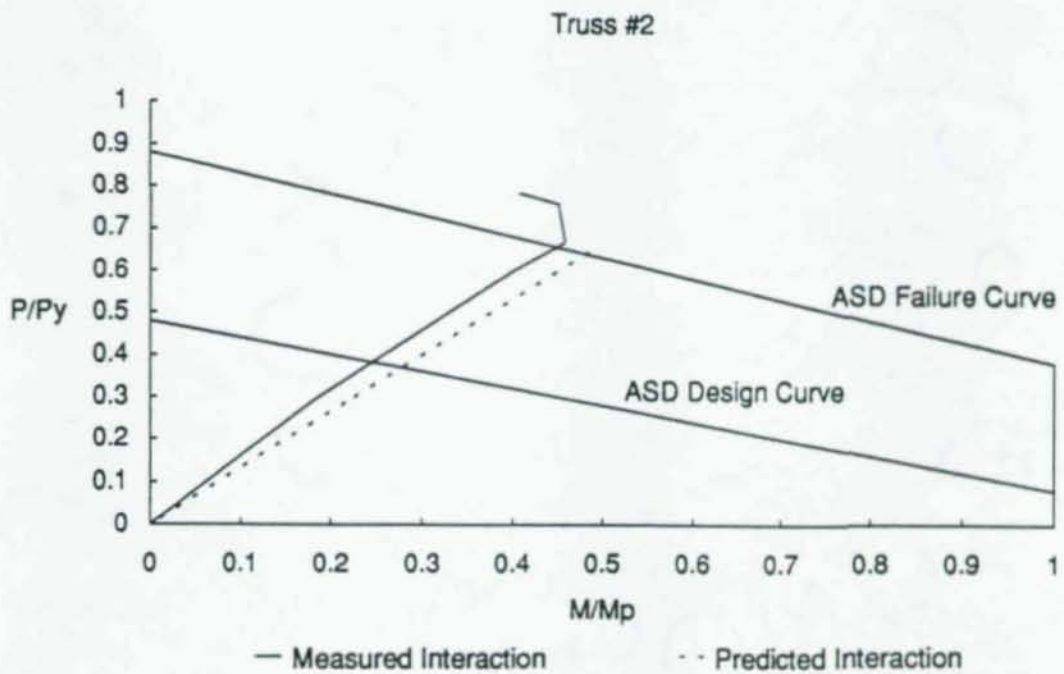
$$\frac{f_a}{0.60F_y} + \frac{f_b}{F_b} \leq 1.0 \quad (4.3)$$

in which

f_a = computed axial stress, (P/A)

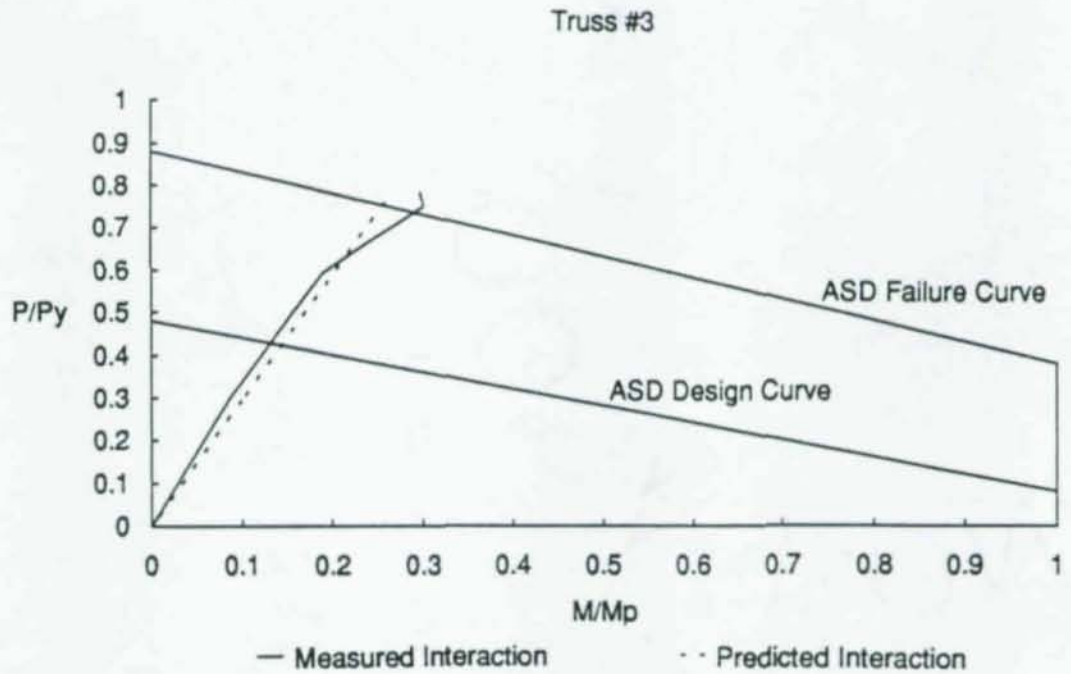


(a)

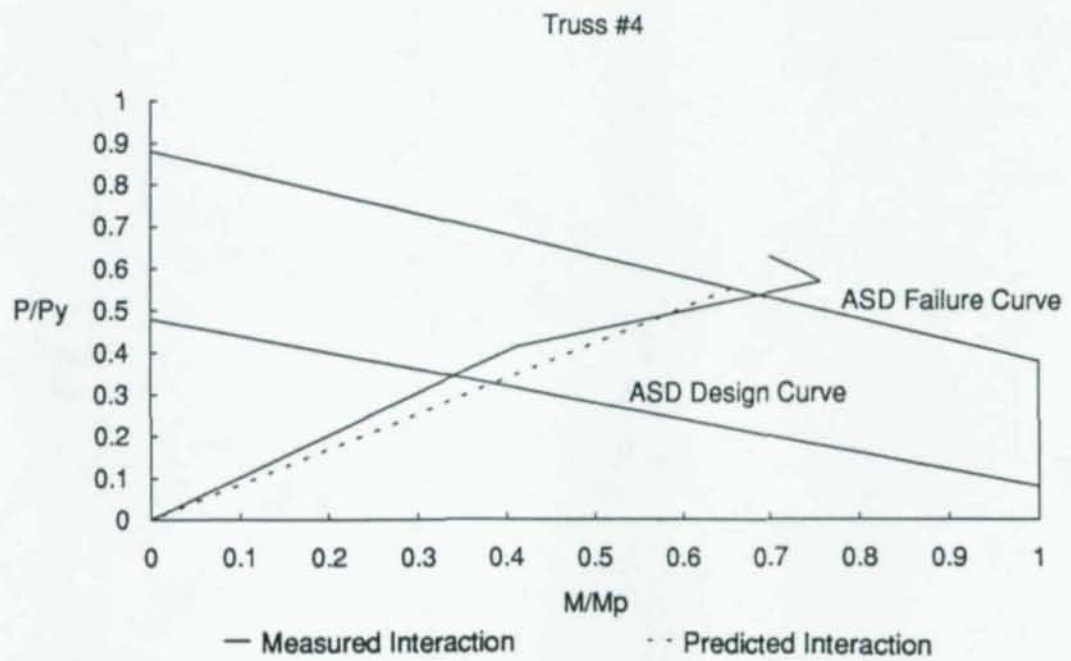


(b)

Figure 4.6 Axial-Moment Interaction Diagrams



(c)



(d)

Figure 4.6 Axial-Moment Interaction Diagrams

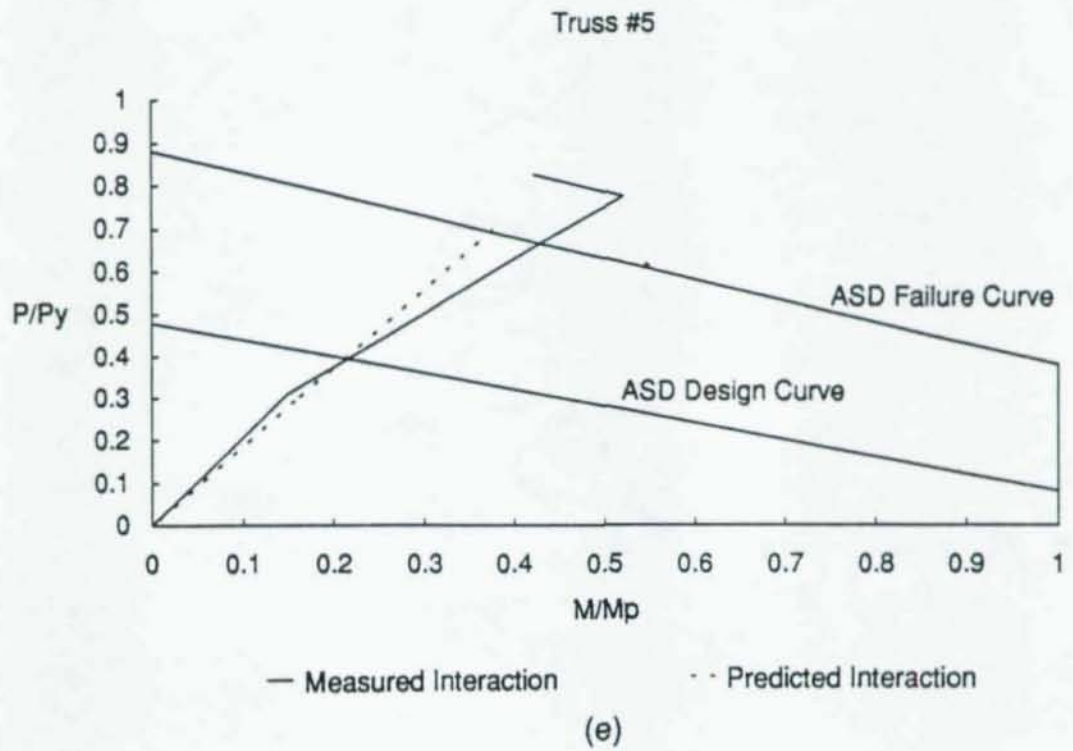


Figure 4.6 Axial-Moment Interaction Diagrams

F_a = allowable compressive stress, for inelastic buckling

$$F_a = \frac{\left[1 - \frac{(KL/r)^2}{2C_c}\right] F_y}{\frac{5}{3} + \frac{3(KL/r)}{8C_c} - \frac{(KL/r)^3}{8C_c^3}}$$

Torsional-flexural buckling was the controlling buckling mode due to the chord members being of intermediate length and a singly symmetric section. Therefore, an equivalent (KL/r) was determined for torsional-flexural buckling using Equation 2.4

f_b = computed compressive bending stress, (MC/I)

F_b = allowable compressive bending stress

$F_b = 0.6F_y$, because the chord was a non-compact section braced laterally at intervals not exceeding $76b_f/\sqrt{F_y}$

F_e = Euler buckling stress divided by a factor of safety

$$F_e = \frac{12\pi^2 E}{23(KL/r)^2}$$

C_m = reduction factor, taken as 1.0 for the chord section U2-U3.

The ASD failure envelope is based on the previous equations with all factors of safety removed. Thus reducing eqns. 4.2 and 4.3 to:

$$\frac{P}{A} + \frac{C_m \left(\frac{MC}{I} \right)}{\left(1 - \frac{P}{F_o} \right) F_y} \leq 1.0 \quad (4.4)$$

and

$$\frac{P}{A} + \frac{\left(\frac{MC}{I} \right)}{F_y} \leq 1.0 \quad (4.5)$$

in which

P = axial load

A = cross-sectional area

F_a = inelastic buckling stress without a factor of safety

$$F_a = \left[1 - \frac{(KL/r)^2}{2C_c^2} \right] F_y$$

torsional-flexural buckling controlled therefore, (KL/r)_o was determined using Equation 2.4

F_o = Euler buckling stress

$$F_o = \frac{\pi^2 E}{(KL/r)^2}$$

M = moment at point of interest

C = distance to extreme compressed fiber

I = moment of inertia about axis of bending

F_y = material yield stress

C_m = reduction factor, taken as 1.0 for the chord section
U2-U3.

The AISC [1986] Load and Resistance Factor Design (LRFD) combined force equations, without load or resistance factors, were also used to predict the failure load. They are as follows:

$$\text{for } \frac{P_u}{F_{cr}} \geq 0.2 \quad \frac{P_u}{F_{cr}} + \frac{8}{9} \left(\frac{M_u C}{I F_y} \right) \leq 1.0 \quad (4.6)$$

$$\text{for } \frac{P_u}{F_{cr}} < 0.2 \quad \frac{P_u}{2F_{cr}} + \left(\frac{M_u C}{I F_y} \right) \leq 1.0 \quad (4.7)$$

in which

A = cross-sectional area

F_y = material yield stress, adequately laterally supported section

F_{cr} = critical buckling stress, torsional-flexural buckling controlled for the critical axial stress as it did in the ASD method, determined using Equations 2.7 & 2.8

P_u = required compressive strength

M_u = required flexural strength

C = distance to extreme compressed fiber

I = moment of inertia about axis of bending.

The average material yield stress for the tee sections of 48.8 ksi was used as the material yield stress within the calculations. The effective slenderness ratio of any unbraced segment, Kl/r , must be defined in order to use Equations 4.2-4.5. For this study, the equivalent column factor K was assumed to be equal to 0.85. This was a compromise between AISC recommended design values for a column with rotationally and translationally fixed end conditions ($K = 0.65$) and a column with rotationally free, translationally fixed end conditions ($K = 1.0$). As joint eccentricities are introduced, the length of the chord member should no longer be taken as the distance between the center line of the connections. However, to assume that the buckling length has been reduced by an equivalent length of eccentricity is unconservative, because some distance into the weld of the joint is required to develop the assumed stiffness. Thus, the length of the beam-column chord sections was conservatively taken as the distance between the theoretical work points of the joints.

The ASD torsional-flexural equations, using the material's actual yield stress of 48.8 ksi and $K = 0.85$, conservatively predicted the failure load for each truss, ranging from 5.8 to 13.6 percent. The use of extreme K factors, $K = 0.65$ and $K = 1.0$, resulted in ultimate loads within 4 percent of those using $K = 0.85$. The LRFD equations were, however, slightly more conservative,

ranging from 7.4 to 15.0 percent.

It appears that the ASD method models the behavior of the truss specimens slightly better than the LRFD method. A singly symmetric section, such as the tee chord, loaded with a bending moment and axial load requires that both positive and negative moments be considered. Due to the large concentration of area in the flange, the magnitude of the extreme fiber stress is significantly different for positive and negative bending moments when combined with an axial load (positive moments correspond to moments producing an increased compression in the flange, and negative moments reduce the flange compression). The ASD combined stress method takes into consideration the magnitude and direction of the bending stress due to the direction of the bending moment on a singly symmetric section. However, the general LRFD combined force equations consider the member strength and must be modified as outlined in section H.2 of the LRFD code [AISC 1986]. Also, when low axial compressive loads and high moments are encountered, tensile yielding at the extreme fiber of the singly symmetric section must be checked.

Local buckling of the tee stem may also become a consideration depending upon the width-thickness ratio of tee stem and the direction and magnitude of the bending moment. Buckling of the stem of the tee chord can be a dominating failure mode if the moment to axial load ratio is high enough as was indicated by the behavior of truss #4. After truss #4 reached its ultimate capacity, the stem of the tee chord U1-U2, adjacent to joint U2,

buckled (see Figure 4.1d).

Bleich [1942] generalized the expression for critical buckling stress of a flat plate segment in either the elastic or inelastic range:

$$\sigma_{cr} = k_c \left(\frac{\pi^2 E_t \sqrt{\eta}}{12(1-\nu^2)(b/t)^2} \right) \quad (4.8)$$

in which k_c is a buckling coefficient that is a function of plate geometry, boundary conditions, and loading, $\eta = E_t/E$, E_t = the tangent modulus, E is Young's modulus, b is the width of the plate, and t is the thickness of the plate. Stresses will vary along the loaded edge of a plate subjected to compressive and bending loads.

Values of k_c have been tabulated by Johnston [1976] for several cases of compression and bending loads. The plasticity reduction factor η is to account for the material's stress-strain relationship, the type of loading, the length-to-width ratio of the plate and the boundary conditions. The plasticity reduction factor, $\eta = E_t/E$, proposed by Bleich is an approximate method used to account for the partial plastification of the plate section.

Calculations were made for the two following cases, assuming the tee flange provided a fixed condition along one edge of the plate element: The first case used $k_c=1.61$ as if the entire section were still elastic, and the second case used $k_c=1.33$ as if full plastification of the section had occurred. The width of the plate was taken as the distance from the tip of the tee stem to the bottom of the flange, 5.75 inches and the thickness of the plate section as 0.30 inches. The stress-strain diagrams from the tensile coupon tests of the tee stem

material were used for the determination of the appropriate tangent modulus. The application of equation 4.8 resulted in a critical stress, σ_{cr} , of 48 ksi for each case. The critical load for member U1-U2 was determined using a moment-to-axial load ratio of 2.845, determined from an elastic analysis of truss #4, for member U1-U2 just outside joint U2. The critical load in the chord stem for the first case, assuming $P/A + MC/I = 48.0$, is $P = 46.2$ kips and $M = 131.4$ inch kips, which translates to an applied load at joint L3 of 87.8 kips, assuming the truss is still fully elastic and the maximum compressive stress is at the tip of the tee stem. The critical load for the second case, assuming a fully plastic section, is $P = 73.8$ kips and $M = 210.1$ inch kips, which translates to an applied load at joint L3 of 140.3 kips.

The values of σ_{cr} for the two cases provide an upper and lower bound for inelastic buckling stress for the chord stem. There are, however, several assumptions within this procedure: 1) The member forces were assumed to remain proportional after the strain in the material had surpassed the proportional limit. A non-linear analysis of the structure could be used to account for the materials non-linearity beyond the proportional limit, but this was beyond the scope of this study; 2) The modified critical buckling stress equation proposed by Bleich (Equation 4.9) is a conservative approximation.

4.4 Truss Stiffness

Experimental and analytical values of overall stiffness are compared in Table 4.3. The truss stiffness was measured as the slope of the linear region

Truss	Truss Stiffness		Percent
	Experimental	Analytical *	Difference
#1	209.9 kip/inch	217.9 kip/inch	-3.8
#2	207.1 kip/inch	204.2 kip/inch	1.4
#3	196.4 kip/inch	205.1 kip/inch	-4.4
#4	173.1 kip/inch	177.8 kip/inch	-2.7
#5	176.9 kip/inch	182.8 kip/inch	-3.3
Perfect Frame		218.7 kip/inch	
Perfect Truss		212.6 kip/inch	

* Analytical values determined using a plane frame analysis

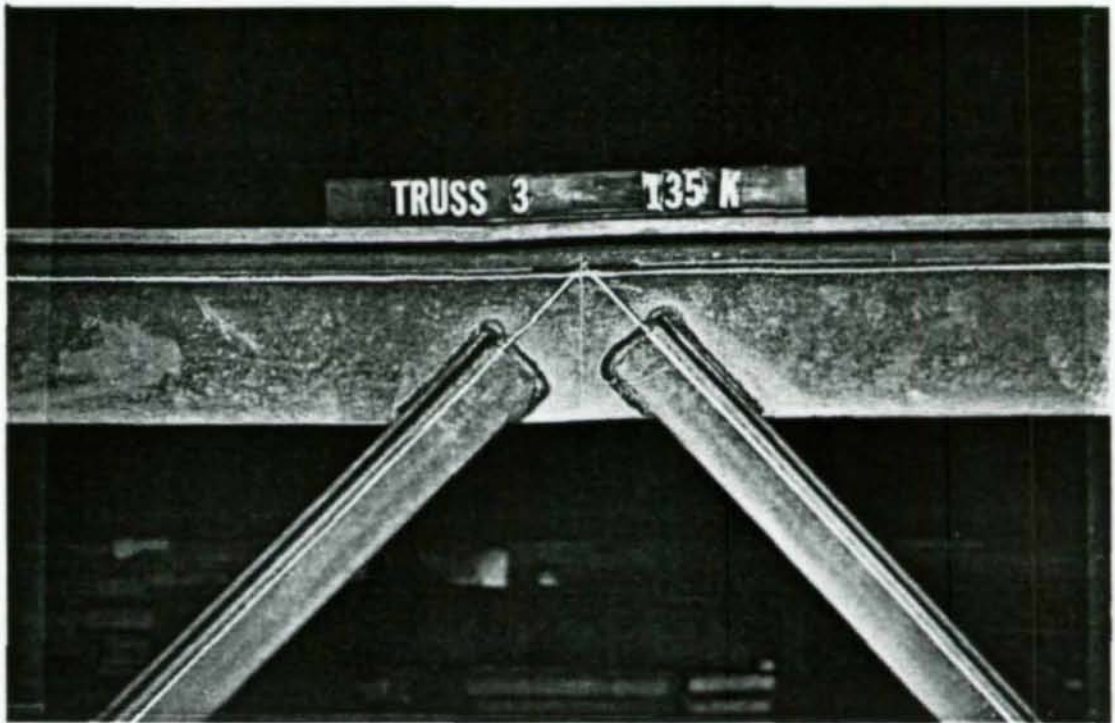
Table 4.3 Truss Stiffness

of the total applied load versus centerline deflection curve (see Figure 4.2). The experimental and analytical values for each truss were within a range of +1.4 to -4.4 percent. However, when comparing the "stiffest" truss, truss #1, with the "softest" truss, truss #4, analytically there was a 21.3 percent loss of stiffness. As was suggested by Dawe and Pond, the joints with larger positive eccentricities did appear to be more ductile, allowing greater deformation for a given load. As can be seen from Figure 4.7, "nearly perfect" joints on the compression and tension chords had little deflection within the joint at the failure load. However, joints shown with positive eccentricities, for both the tension and compression chords, had noticeable displacements within the joint.

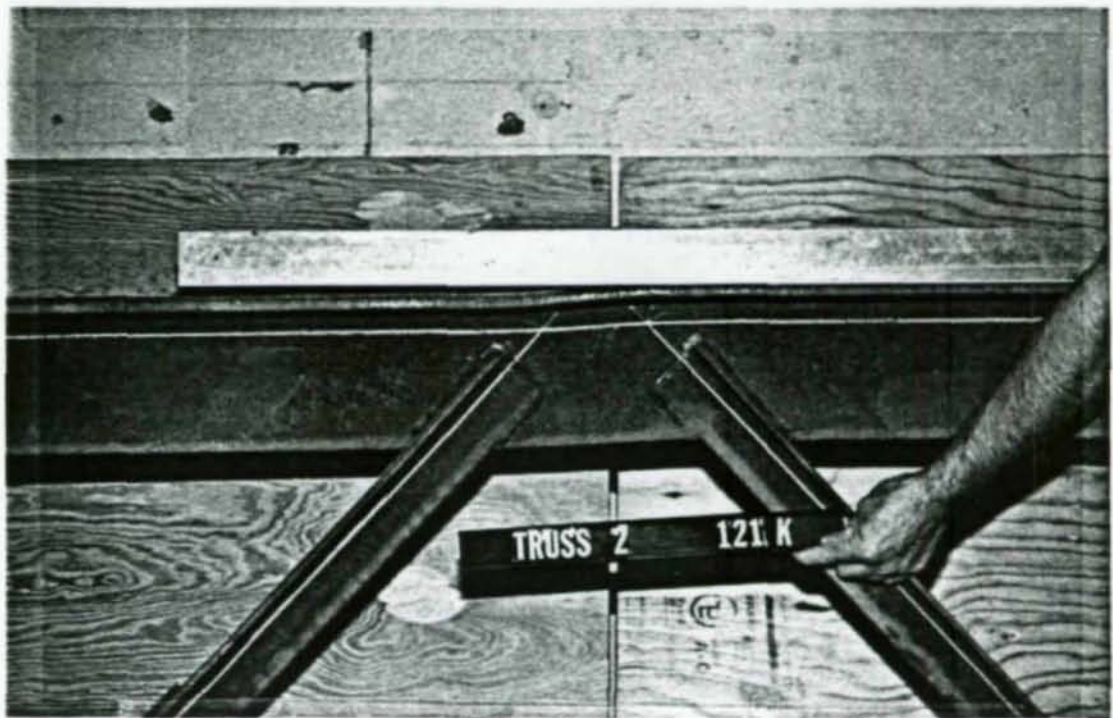
4.5 Conclusions

As shown in Figures 4.6 and Table 4.2, a plane frame analysis considering moment, axial, and shear forces closely predicts the ultimate capacity of the truss. The member end forces were closely predicted by the plane frame analysis, as were the axial and shear forces within the joint. The moments within the joints appeared to be dependent upon the placement and location of the web members on the stem of the tee chord.

The buckling failures of the truss specimens were above that predicted by the ASD analysis, varying from 5.8 percent to 13.6 percent, when the material's average yield stress of 48.8 ksi was used. Thus, it would seem that the AISC ASD stability formula results in a satisfactory design and the truss



(a) Concentric Top Chord Joint



(b) Eccentric Top Chord Joint

Figure 4.7 a & b Typical Joint Distortion

specimens at failure come very close to the factor of safety predicted by the formula. This agrees with the observations and predicted performance proposed by Lenzen and Korol et al. [1986] as to the adequacy of the Allowable Stress Design combined stress stability equation.

The truss specimens with large positive joint eccentricities had lower ultimate load carrying capacity and overall stiffness than trusses without joint eccentricities. Consideration must, however, be given to member forces when comparing the behavior of the tension joints (L2 and L4) and compression joints (U2 and U3). Although the joints were constructed of identical members aligned in similar geometry, the member forces when comparing the tension joints with the compression joints were not the same. That is, while the shear load transferred within joints L2, L4, U2, and U3 was the same magnitude for a given applied load, the axial load was not (see Figure 3.1). Also, the tension chord was oversized, thus the effects of positive joint eccentricities on the ultimate capacity of the tension chord members were not observed. Therefore, no direct comparison of the effects of joint eccentricities on the tension and compression chord is made. The test specimens with joint eccentricities on the tension chord did serve to help model and analyze the effects that positive joint eccentricities on the tension chord have on compression members within the truss.

Conclusions and Recommendations

5.1 Summary and Conclusions

A test plan, fixtures, and procedures to study the behavior of planar trusses with misaligned members were defined, developed, and conducted in this thesis. The test results were analyzed and compared with analytic models and design procedures.

The following conclusions can be made based on the test results and analysis described in this report.

1) Based on the results from the "perfect" truss, a truss with a two inch eccentricity on the compression chord had a 13 percent reduction of load carrying capacity and a 1.3 percent loss of overall stiffness and a truss with a four inch eccentricity on the compression chord had a 21 percent reduction of load carrying capacity with a 17.5 percent loss of overall stiffness. Therefore, stresses due to positive eccentricities at the panel points of a truss can have a significant effect on the behavior and capacity of a planar "truss" structure.

2) The two primary influential factors for the truss configuration investigated were the magnitude of the eccentricity and the magnitude of the shear load transferred through the connection due to the vertical force component in the diagonal web members. This truss configuration had high

diagonal forces, therefore, it is expected that these results are conservative for a truss with higher span length to depth ratios.

3) The computer model, a plane frame analysis, closely estimated the *member end forces for the truss specimens tested.*

4) Axial and shear forces within the connections were accurately predicted by the plane frame analysis. However, to predict the moment forces within the connections a more sophisticated analysis of the joint would be necessary. The actual moment forces within the connection appeared to be dependent on the depth of placement of the web members along the stem of the tee section.

5) The ASD combined stress analysis satisfactorily predicted the ultimate capacity of the chord member U2-U3, within the range of 5.8 to 13.6 percent conservative, when the material's actual yield stress of 48.8 ksi was used. The LRFD combined force analysis, however, was slightly more conservative, ranging from 7.4 to 15.0 percent. The magnitude and direction of the bending stress due to the direction of the bending moment on a singly symmetric section combined with axial stresses, must be considered when using either method. The results for both methods were similar when section H.2 of the LRFD code is considered [AISC 1986].

6) The results of the four inch eccentric joint on the compression chord, truss #4, indicated that stem buckling of the tee chord could become critical, depending upon the direction and magnitude of the axial and bending stresses.

5.2 Design and Analysis Recommendations

Trusses constructed of tee sections for the top and bottom chords with double angle web members fastened directly to the stem of the tee chord are commonly used due to the ease of construction and economy of the structure. However, truss systems that are designed based on the assumption of having concentrically loaded joints, may in fact have eccentricities that need to be evaluated. Based on the results of this thesis, positive joint eccentricities of sufficient magnitude were found to have a detrimental effect on truss strength and stiffness. Thus, the influence of the positive joint eccentricity on the member design forces must be evaluated. Any rational design approach must be based on not only axial member forces, but also shear and moment member forces when evaluating joint eccentricities.

The following are design considerations and recommendations to be kept in mind when analyzing and/or designing truss systems with positive eccentric joints:

(1) The analytic model used to represent a structure must consider all primary member forces involved. Thus, when joint eccentricity is present due to member misalignment, the axial, shear, and moment forces induced by the eccentricity as well as any changes to the member axial force must be modeled.

(2) A reasonable approach to determine member forces of a truss with eccentric joints is to model the chord as a continuous member with the web members connected at their respective intersection points along the chord. All

resulting stresses should be treated as primary stresses.

(3) The actual effective length of the truss chord member was difficult to determine because of the welding at the joint. It would appear that the effective length is less than the distance between panel points, but greater than the clear distance between the ends of the joint welds. The joint rigidity and relative stiffness of the truss chords must be considered when determining the member's effective length.

(4) The axial force-moment interaction for each member must be evaluated when the member forces are determined using a "frame" model.

(5) Because of the loads induced in a top chord due to joint eccentricity, the negative bending causing compression in the stem of the tee section must be considered.

(6) Web members are often fastened as close to the tip of the tee stem as possible in order to provide a concentric connection and still provide adequate effective weld length to develop the connection. However, web members should be placed deeper in the tee section in order to spread out the shear stresses. AISC allows a shear stress of $0.40 F_y$ to be applied over the full area of the beam web, but judgment should be used in cases where the connection length is considerably less than the depth of the beam [AISC 1989].

5.3 Recommendations for Further Work

Further research should be conducted to provide additional engineering data related to trusses with eccentric connections. The number of variables

considered in this study were limited and, therefore, additional information is needed.

Trusses with eccentric connections in conjunction with roof and floor systems need to be tested. This type of research would yield information about the effect of the roof or floor system on the truss strength and stiffness. The effect of fatigue type loading on eccentric trusses deserves special consideration. In addition, the effect of positive joint eccentricity on the ultimate strength of the tension chord and web members should be investigated.

References

American Institute of Steel Construction. (1986). *Manual of Steel Construction Load & Resistance Factor Design*. 1st ed., American Institute of Steel Construction, Inc., Chicago, Illinois.

American Institute of Steel Construction. (1989). *Manual of Steel Construction Allowable Stress Design*. 9th ed., American Institute of Steel Construction, Inc., Chicago, Illinois.

ASTM (1989). "Mechanical Testing of Steel Products," (ASTM A 370-77) 1989 *Annual Book for ASTM Standards*, Vol 03.01, American Society for Testing and Materials, Philadelphia, PA, pp. 3-48.

Bleich, F. (1952). *Buckling Strength of Metal Structures*. McGraw-Hill Book Co., Inc., New York, N.Y.

Celestial Software, Inc. (1988). *IMAGES-3D Finite Element Analysis Program User's Manual*, Berkley, CA.

Dawe, J.L., Pond, B.S., and Grondin, G.Y. (1985). "Interaction of Shear and Tension in Welded Truss Connections." *Can. J. Civ. Eng.*, Vol. 12, pp. 94-103.

Gibson, G.J., and Wake, B.T. (1942). "An Investigation of Welded Connections for Angle Tension Members." *Welding J., J. Amer. Welding Soc.*, Welding Res. Supplement, Vol.21 No. 1, pp. 44s-49s.

Johnston, B.G. (1976). *Guide to Stability Design Criteria for Metal Structures*, 3rd ed., John Wiley & Sons, New York, N.Y.

Kennedy, J.B., Murty, M.K.S. (1972). "Buckling of Steel Angle and Tee Struts." *J. Struct. Div. ASCE*, Vol. 98 No.ST11, pp. 2507-2522.

Korol, R.M., Rutenberg, A., and Bagnariol D. (1986). "On Primary and Secondary Stresses in Triangulated Trusses." *J. Construct. Steel Research*, Vol. 6 No. 2, pp. 123-142.

Lenzen K.H. (1968). *Final Report Design Formulas for the Top Chords of Open-Web Steel Joists*. The University of Kansas Center for Research Inc., Studies in Engineering Mechanics, Report Number 27.

Measurements Group Tech Note, TN-515. (1990) "*Strain Gage Rosettes - Selection, Application and Data Reduction*", Measurements Group Inc., Raleigh, North Carolina.

Nair, R.S. (1988). "Secondary Stresses in Trusses." *Engineering Journal*, American Institute of Steel Construction, Vol. 25 No. 4, p. 144.

Parcel, J.I., and Murer, E.B. (1936). "Effect of Secondary Stresses Upon Ultimate Strength." *Trans. ASCE*, Vol. 101, pp. 289-343.

Salmon, C.G., and Johnson, J.E. (1980). *Steel Structures Design and Behavior*. 2nd ed., Harper & Row, New York, N.Y.

Timoshenko, S. (1966). *Strength of Materials Part II Advanced Theory and Problems*. 3rd ed., D. Van Nostrand Co., Inc., Princeton, New Jersey.

Walton, B.A. (1979). "Interaction of Shear and Tension in Welded Truss Connections." *Can. J. Civ. Eng.*, Vol. 6, pp. 567-574.

West, H.H. (1989). *Analysis of Structures*. 2nd ed., John Wiley & Sons, New York, N.Y.

Willems N., Easley J.T., and Rolfe S.T. (1981). *Strength of Materials*. McGraw-Hill Book Co., Inc., New York, N.Y.

